Supplement of Atmos. Meas. Tech., 18, 7421–7444, 2025
https://doi.org/10.5194/amt-18-7421-2025-supplement

Atmospheric Measurement Techniques
Open Access

Supplement of

New quantitative measurements and spectroscopic line parameters of ammonia in the 685–1250 cm^{-1} spectral region for atmospheric remote sensing

Daniel J. L. Coxon et al.

Correspondence to: Daniel J. L. Coxon (djlc1@leicester.ac.uk) and Jeremy J. Harrison (jh592@leicester.ac.uk)

Supporting Information

S1 Data comparison plots

S1.1 $\nu_2(a) \leftarrow GS(s)$ Q branch plots

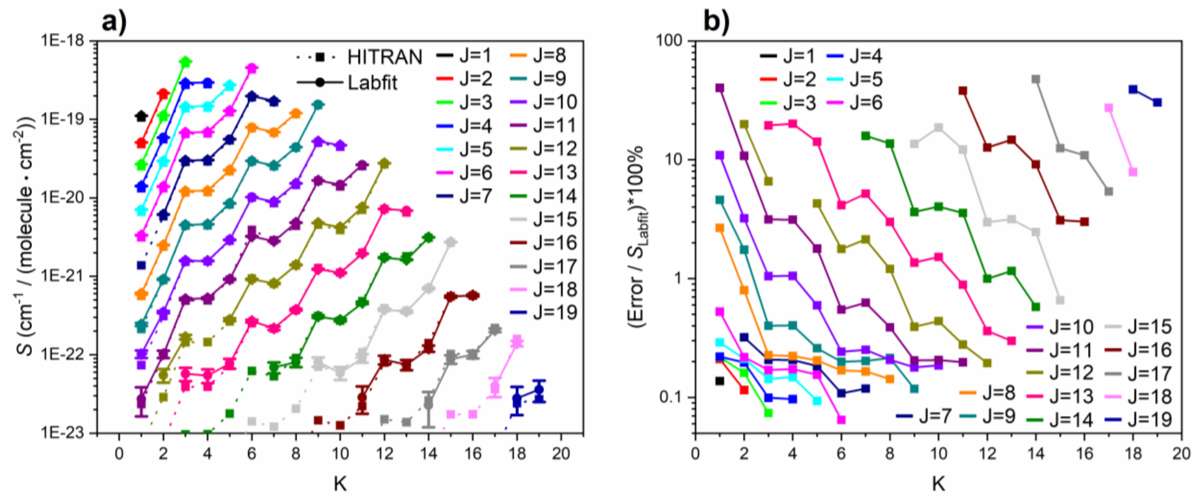

Figure S1. Plots of (a) spectral line intensity S, with Labfit value uncertainties of 3σ, and (b) 3σ uncertainty divided by Labfit line intensity S_{Labfit} plotted against K for each J value of the NH_3 $\nu_2(a) \leftarrow GS(s)$ Q branch.

S1.2 $\nu_2(s) \leftarrow GS(a)$ Q branch plots

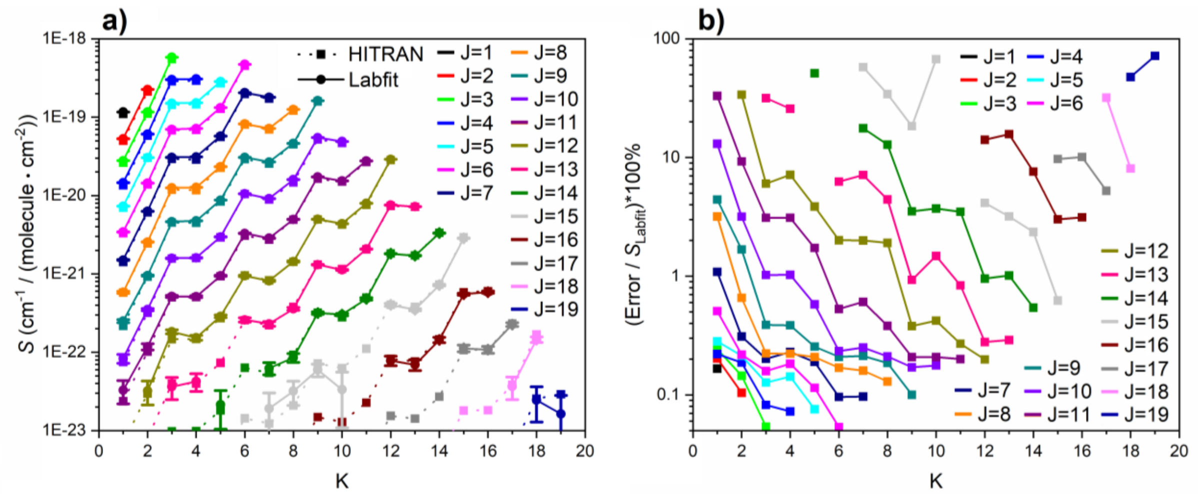

Figure S2 Plots of (a) spectral line intensity S, with Labfit value uncertainties of 3σ (b) 3σ uncertainty divided by Labfit line intensity S_{Labfit} plotted against K for each J value of the NH_3 $\nu_2(s) \leftarrow GS(a)$ Q branch.

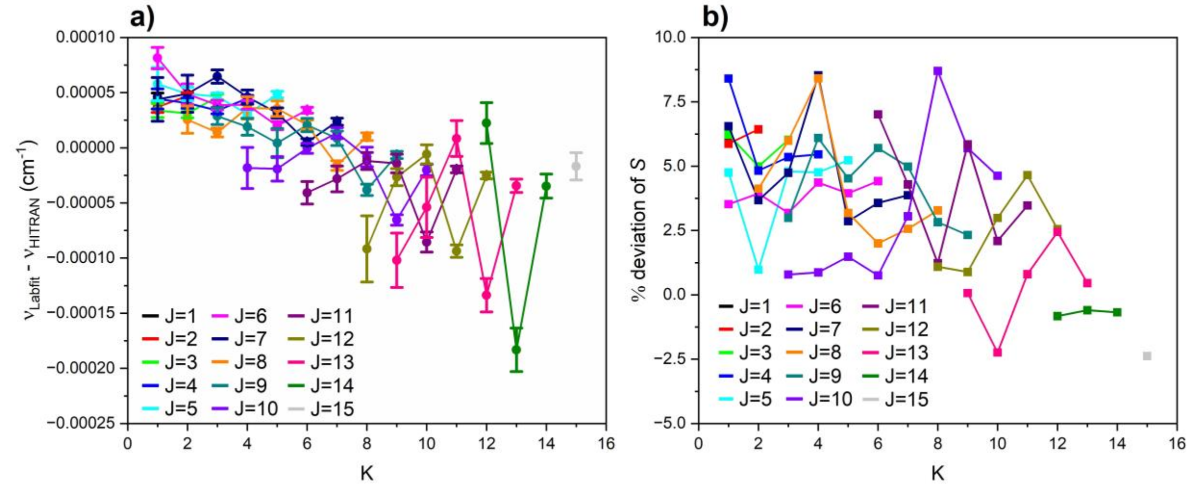

Figure S3. (a) Differences between the measured line positions and those from HITRAN 2020 for the NH_3 $\nu_2(s) \leftarrow GS(a)$ Q branch lines, and (b) percentage deviations in intensity between the measured line intensities and those from HITRAN 2020 for the NH_3 $\nu_2(s) \leftarrow GS(a)$ Q branch lines. For both cases, only lines with line intensity > 1 x 10^{-21} cm^{-1} / (molecule cm^{-2}) are plotted, and the error bars are 3σ.

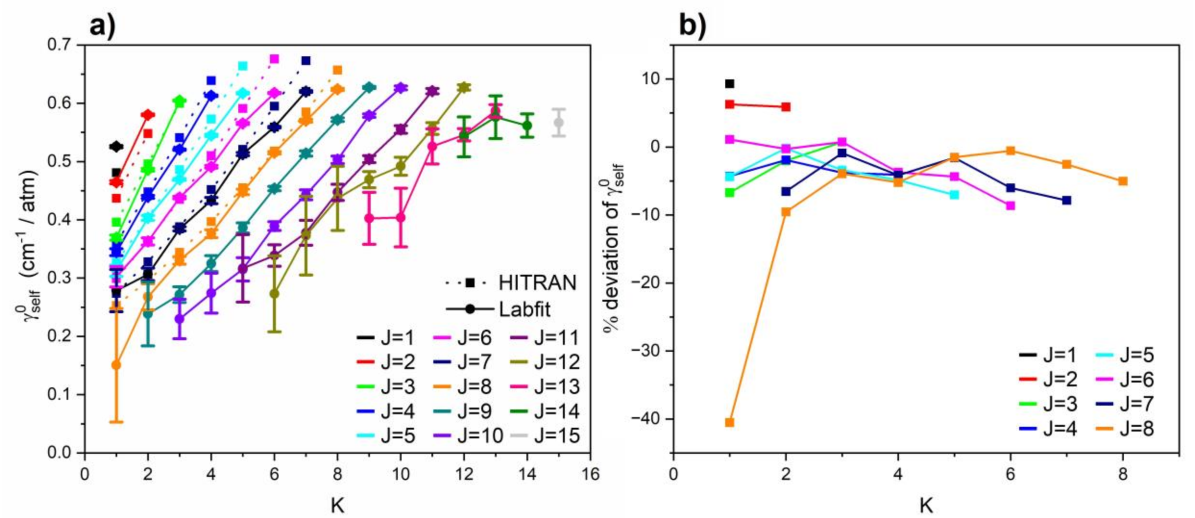

Figure S4. Plots of (a) self-broadened halfwidth, γ^0_{self}, and (b) percentage deviations from HITRAN of γ^0_{self} plotted against K for each J value of the $\nu_2(s) \leftarrow GS(a)$ Q branch. The Labfit values are included with uncertainties of 3σ. For J > 8, HITRAN values for the self-broadened halfwidth were all set to 0.5, so percentage deviations have not been calculated for these cases.

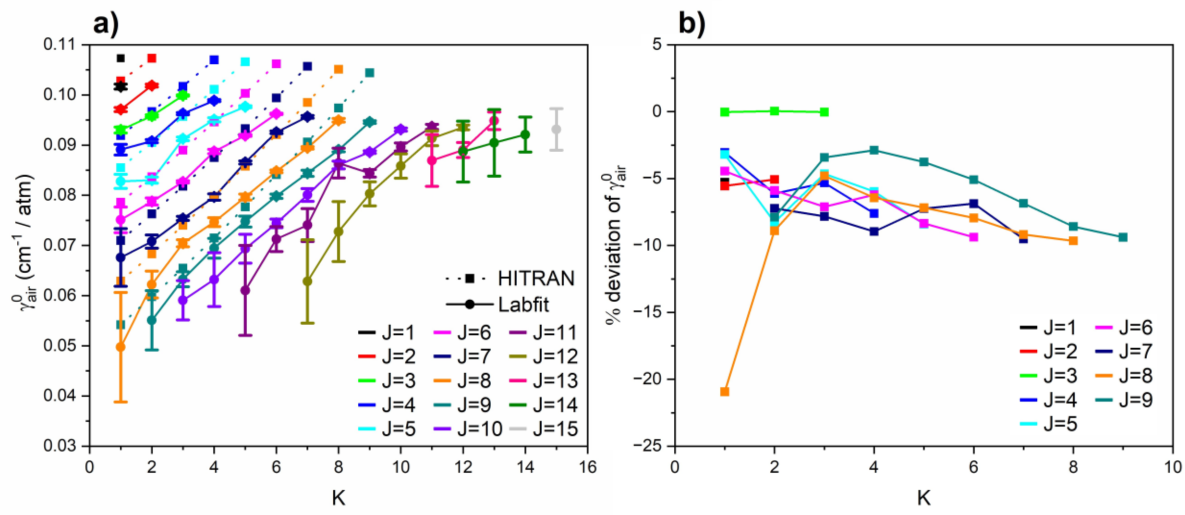

Figure S5. Plots of (a) air-broadened halfwidth, γ^0_{air}, and (b) percentage deviations from HITRAN of γ^0_{air} plotted against K for each J value of the $\nu_2(s) \leftarrow GS(a)$ Q branch. The Labfit values are included with uncertainties of 3σ. For J > 9, HITRAN values for the air-broadened halfwidth were set to the same value as their corresponding K value at J = 9 (with values of K > 9 set to the value for K = 9), so percentage deviations have not been calculated for these cases.

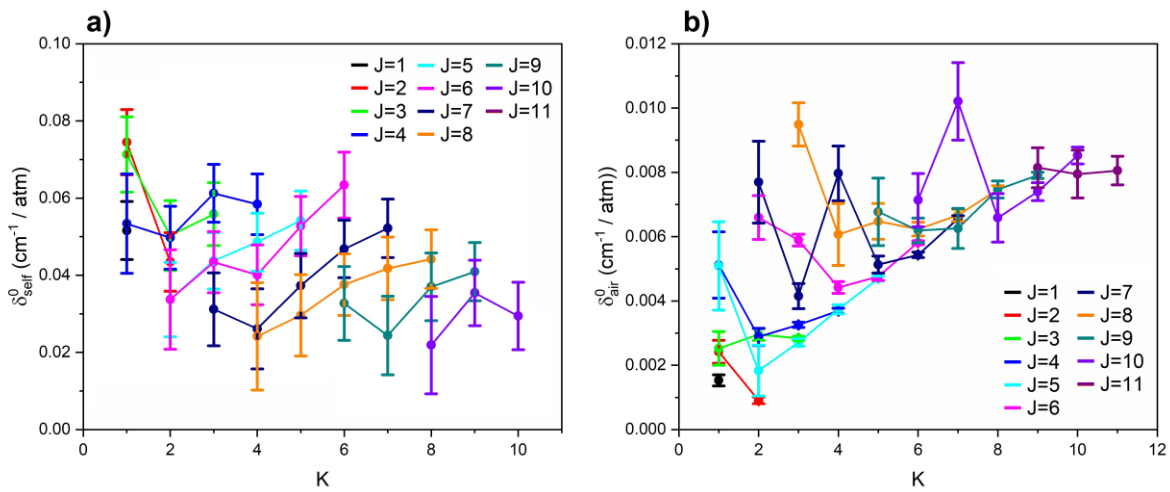

Figure S6. Plots of (a) self-pressure-induced shifts, δ^0_{self}, and (b) air-pressure-induced shifts, δ^0_{air}, against K for each J value of the $\nu_2(s) \leftarrow GS(a)$ Q branch. Measured values are plotted with uncertainties of 3σ. The HITRAN 2020 database does not include values for these parameters.

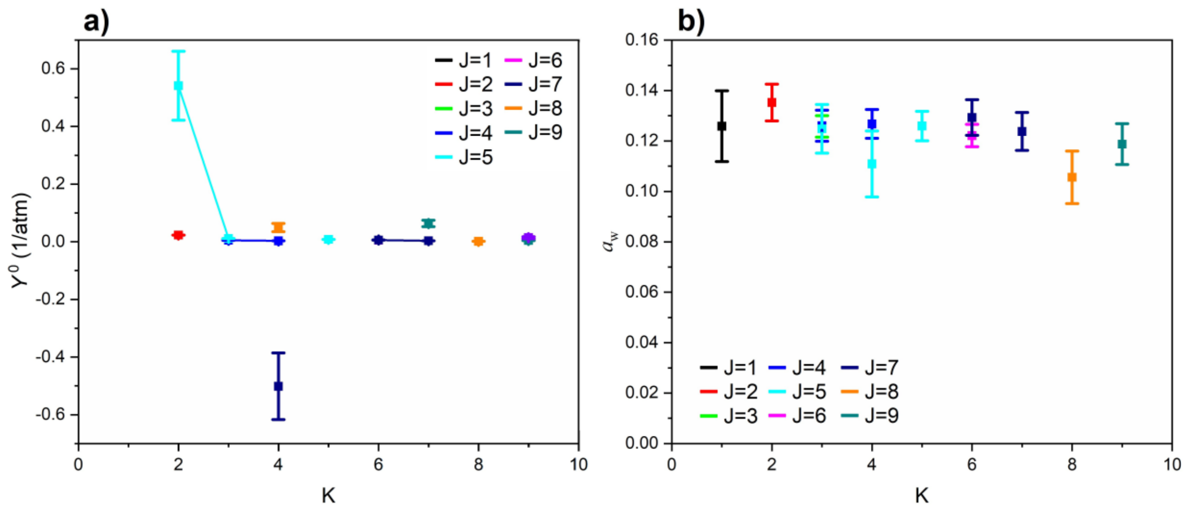

Figure S7. Plots of (a) Rosenkranz line mixing parameter, Y_{air}^0, and (b) speed dependence of the halfwidth parameter, $a_w(air)$, against K for each J value of the $\nu_2(s) \leftarrow GS(a)$ Q branch. The present measured values are shown with uncertainties of 3σ. The HITRAN 2020 database does not include values for these line parameters of NH_3.

S1.3 $\nu_2(a) \leftarrow GS(s)$ P branch plots

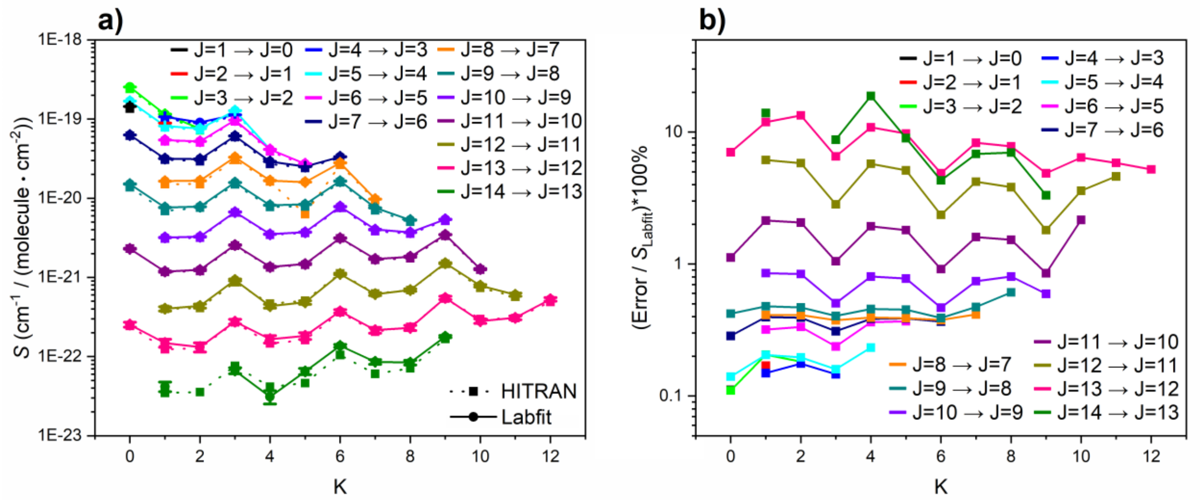

Figure S8. Plots of (a) spectral line intensity S, with Labfit value uncertainties of 3σ, and (b) 3σ uncertainty divided by Labfit line intensity S_{Labfit} plotted against K for each J value of the NH_3 $\nu_2(a) \leftarrow GS(s)$ P branch.

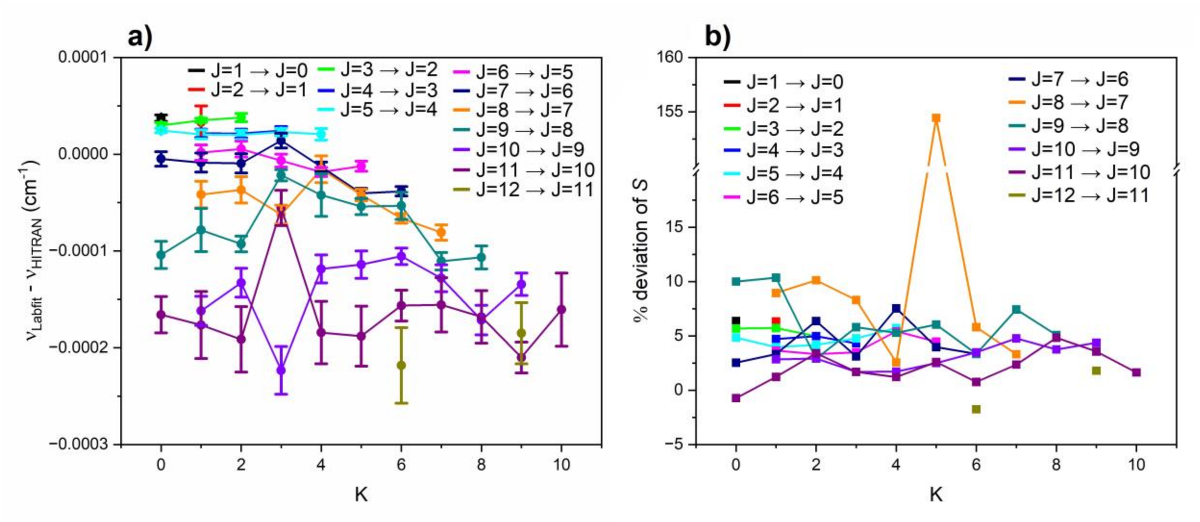

Figure S9. (a) Differences between the measured line positions and those from HITRAN 2020 for the NH_3 $\nu_2(a) \leftarrow GS(s)$ P branch lines, and (b) percentage deviations in intensity between the measured line intensities and those from HITRAN 2020 for the NH_3 $\nu_2(a) \leftarrow GS(s)$ P branch lines. For both cases, only lines with line intensity > 1 x 10^{-21} cm^{-1} / (molecule cm^{-2}) are plotted, and the error bars are 3σ.

The ratio between the Labfit value and the HITRAN 2020 value for the spectral line intensity of the line at J" = 8, K = 5 is the outlier of the plot in **Figure S9b**, with its value being more than twice that of any other intensity ratio. As shown in **Figure S8a**, the HITRAN 2020 value does not at all fit with the trend in line intensities for the other lines at K = 5, which are normally close in value to the spectral line intensity of K = 4 for the same J". The new Labfit line intensity fits the expected trend.

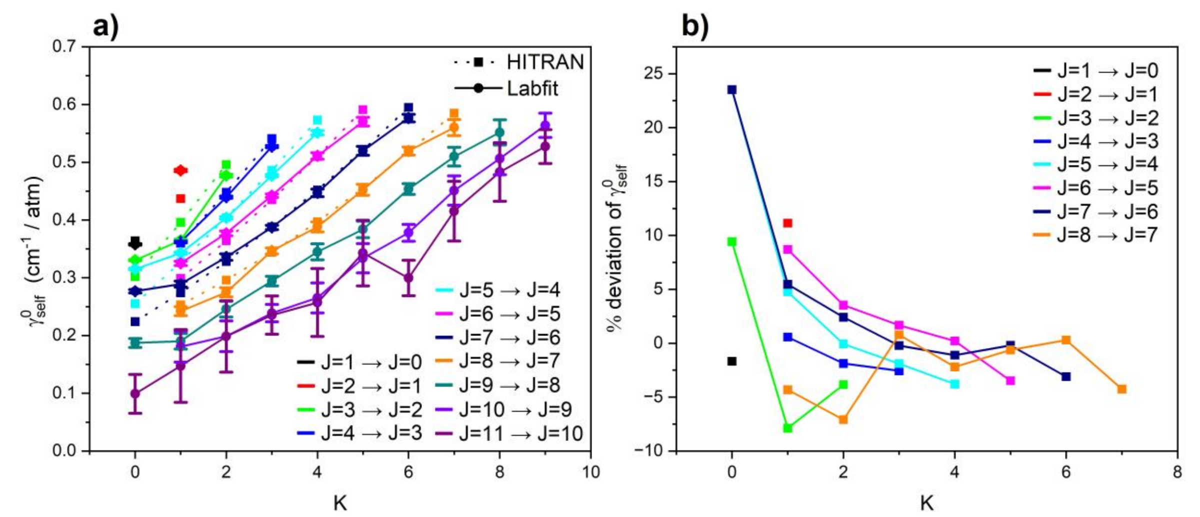

Figure S10. Plots of (a) self-broadened halfwidth, γ^0_{self}, and (b) percentage deviations from HITRAN of γ^0_{self} plotted against K for each J value of the $\nu_2(a) \leftarrow GS(s)$ P branch. The Labfit values are included with uncertainties of 3σ. For J" > 8, HITRAN values for the self-broadened halfwidth were all set to 0.5, so percentage deviations have not been calculated for these cases.

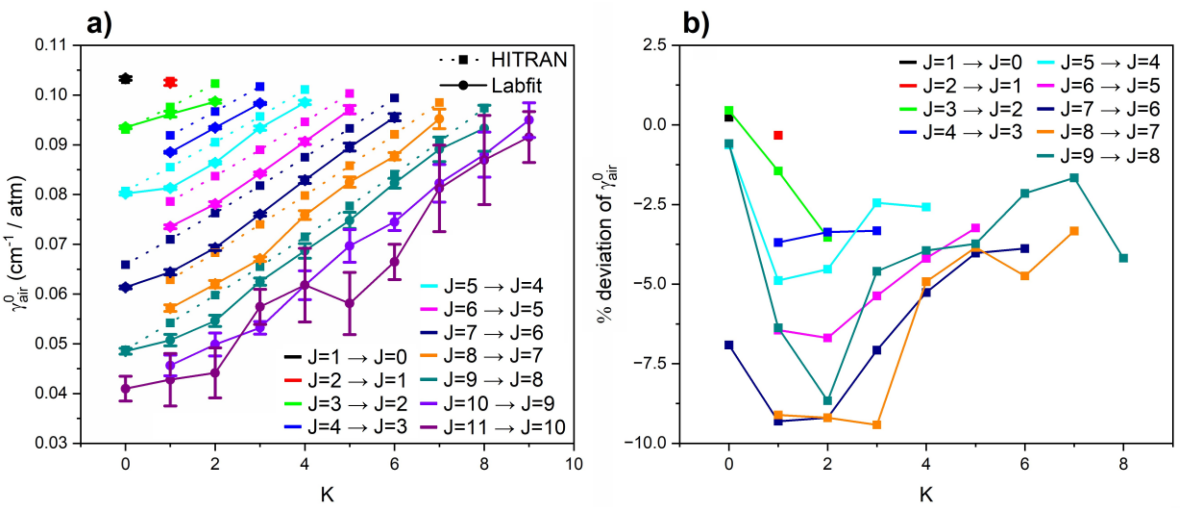

Figure S11. Plots of (a) air-broadened halfwidth, γ_{air}^0, and (b) percentage deviations from HITRAN of γ_{air}^0 plotted against K for each J value of the $\nu_2(a) \leftarrow GS(s)$ P branch. The Labfit values are included with uncertainties of 3σ. For J" > 9, HITRAN values for the air-broadened halfwidth were set to the same value as their corresponding K value at J" = 9 (with values of K > 9 set to the value for K = 9), so percentage deviations have not been calculated for these cases.

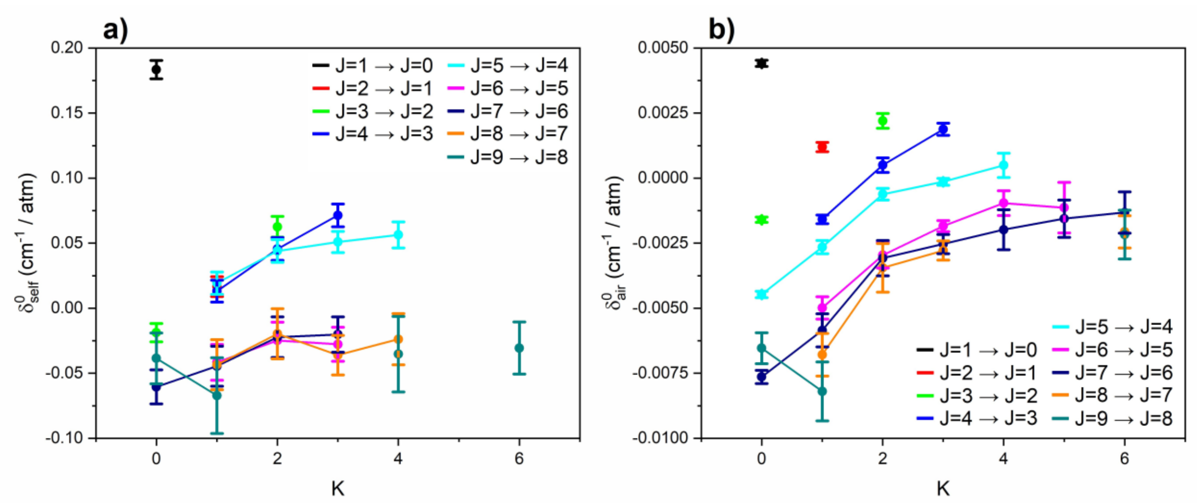

Figure S12. Plots of (a) self-pressure-induced shifts, δ_{self}^0, and (b) air-pressure-induced shifts, δ_{air}^0, against K for each J value of the $\nu_2(a) \leftarrow GS(s)$ P branch. Measured values are plotted with uncertainties of 3σ. The HITRAN 2020 database does not include values for these parameters.

S1.4 $\nu_2(s) \leftarrow GS(a)$ P branch plots

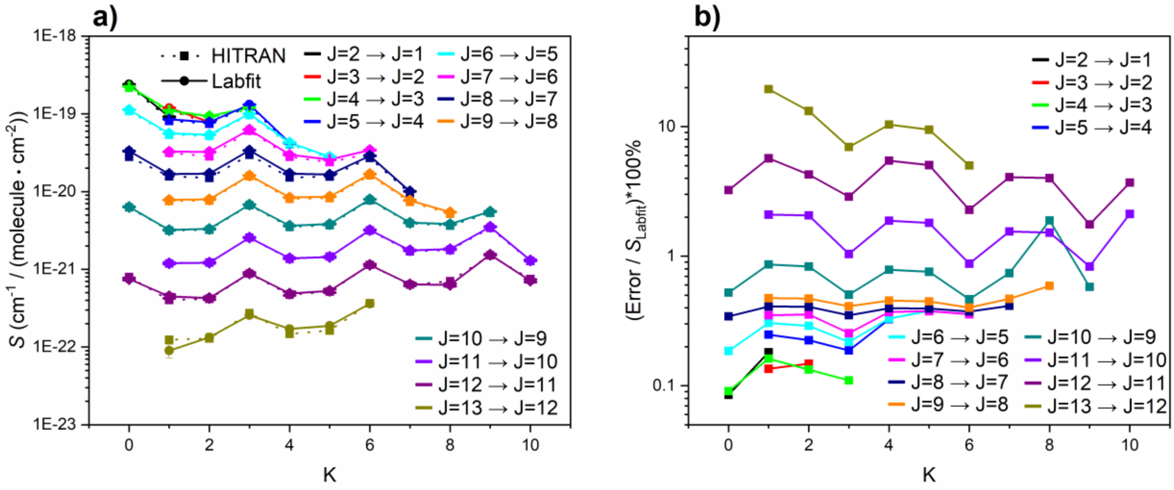

Figure S13. Plots of (a) spectral line intensity S, with Labfit value uncertainties of 3σ, and (b) 3σ uncertainty divided by Labfit line intensity S_{Labfit} plotted against K for each J value of the NH_3 $\nu_2(s) \leftarrow GS(a)$ P branch.

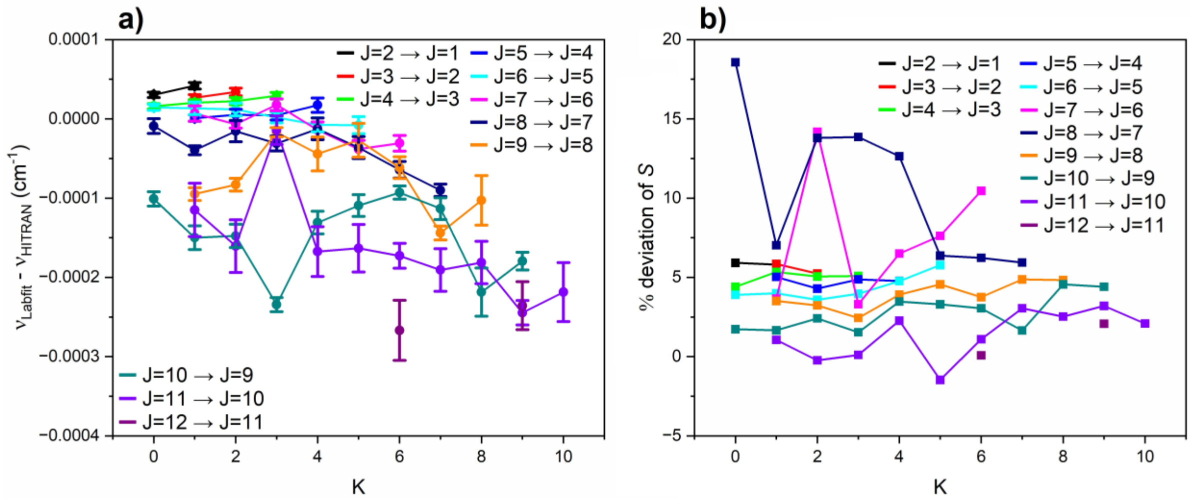

Figure S14. (a) Differences between the measured line positions and those from HITRAN 2020 for the NH_3 $\nu_2(s) \leftarrow GS(a)$ P branch lines, and (b) percentage deviations in intensity between the measured line intensities and those from HITRAN 2020 for the NH_3 $\nu_2(s) \leftarrow GS(a)$ P branch lines. For both cases, only lines with line intensity > 1 x 10^{-21} cm^{-1} / (molecule cm^{-2}) are plotted, and the error bars are 3σ.

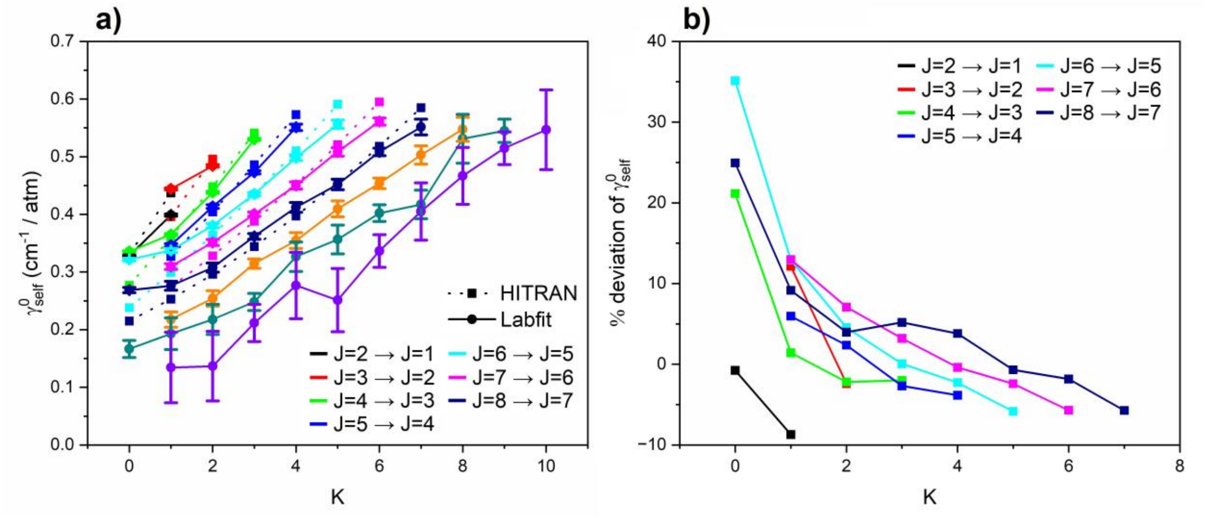

Figure S15. Plots of (a) self-broadened halfwidth, γ^0_{self}, and (b) percentage deviations from HITRAN of γ^0_{self} plotted against K for each J value of the $\nu_2(s) \leftarrow GS(a)$ P branch. The Labfit values are included with uncertainties of 3σ. For J” > 8, HITRAN values for the self-broadened halfwidth were all set to 0.5, so percentage deviations have not been calculated for these cases.

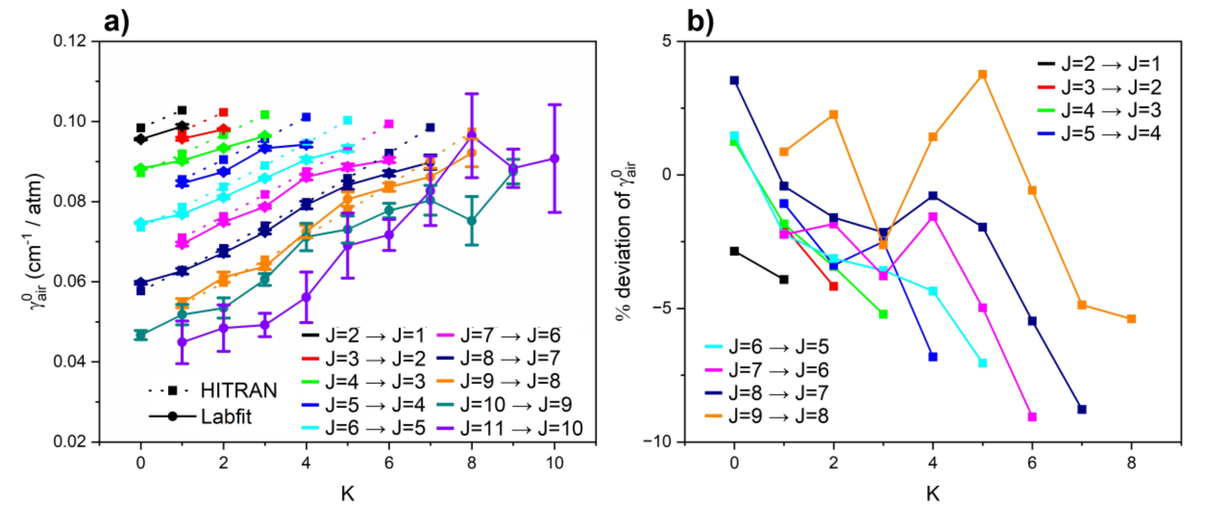

Figure S16. Plots of (a) air-broadened halfwidth, γ^0_{air}, and (b) percentage deviations from HITRAN of γ^0_{air} plotted against K for each J value of the $\nu_2(s) \leftarrow GS(a)$ P branch. The Labfit values are included with uncertainties of 3σ. For J” > 9, HITRAN values for the air-broadened halfwidth were set to the same value as their corresponding K value at J” = 9 (with values of K > 9 set to the value for K = 9), so percentage deviations have not been calculated for these cases.

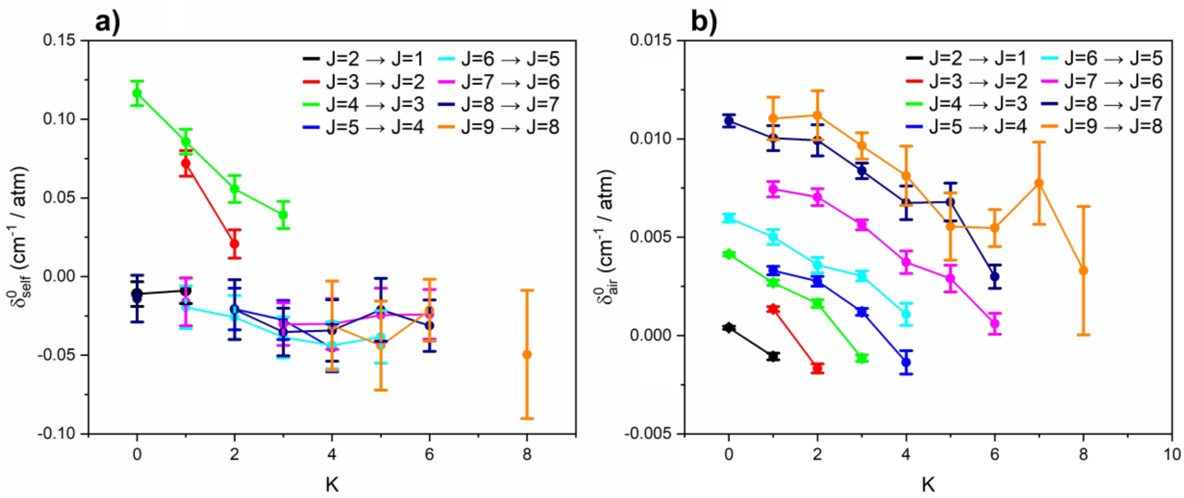

Figure S17. Plots of (a) self-pressure-induced shifts, δ^0_{self}, and (b) air-pressure-induced shifts, δ^0_{air}, against K for each J value of the $\nu_2(s) \leftarrow GS(a)$ P branch. Measured values are plotted with uncertainties of 3σ. The HITRAN 2020 database does not include values for these parameters.

S1.5 $\nu_2(a) \leftarrow GS(s)$ R branch plots

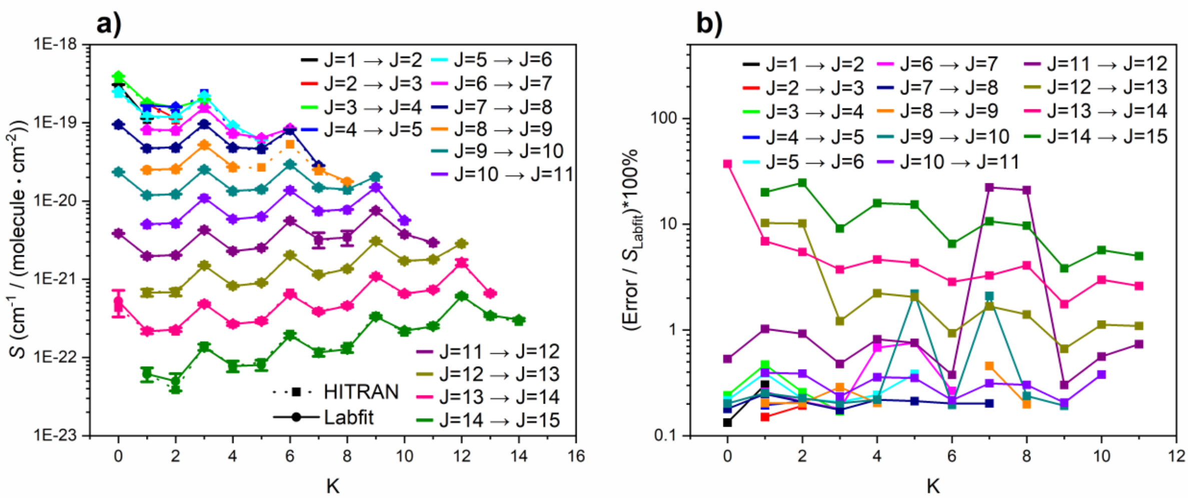

Figure S18. Plots of (a) spectral line intensity S, with Labfit value uncertainties of 3σ, and (b) 3σ uncertainty divided by Labfit line intensity S_{Labfit} plotted against K for each J value of the NH_3 $\nu_2(a) \leftarrow GS(s)$ R branch.

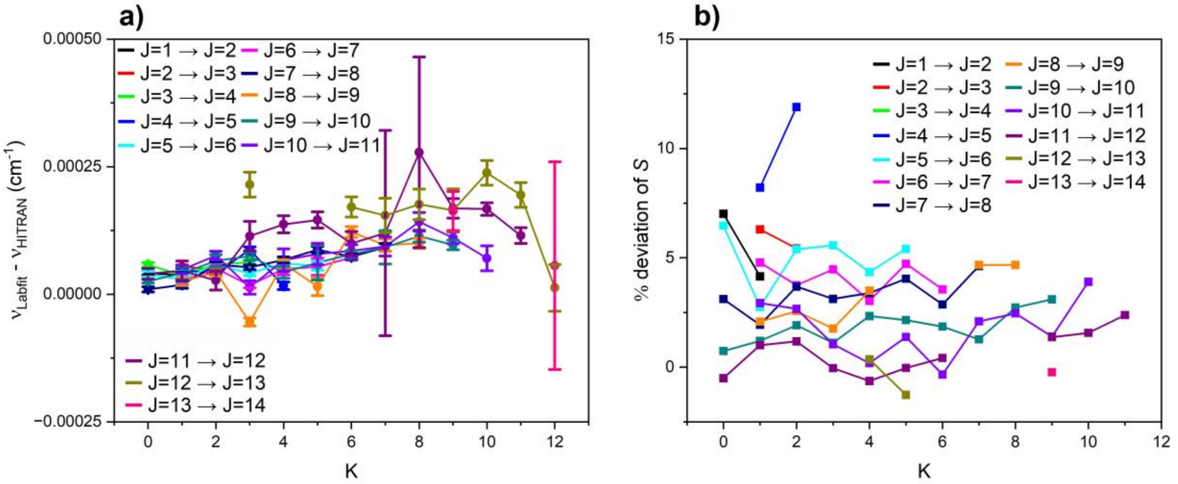

Figure S19. (a) Differences between the measured line positions and those from HITRAN 2020 for the NH_3 $\nu_2(a) \leftarrow GS(s)$ R branch lines, and (b) percentage deviations in intensity between the measured line intensities and those from HITRAN 2020 for the NH_3 $\nu_2(a) \leftarrow GS(s)$ R branch lines. For both cases, only lines with line intensity > 1 x 10^{-21} cm^{-1} / (molecule cm^{-2}) are plotted, and the error bars are 3σ.

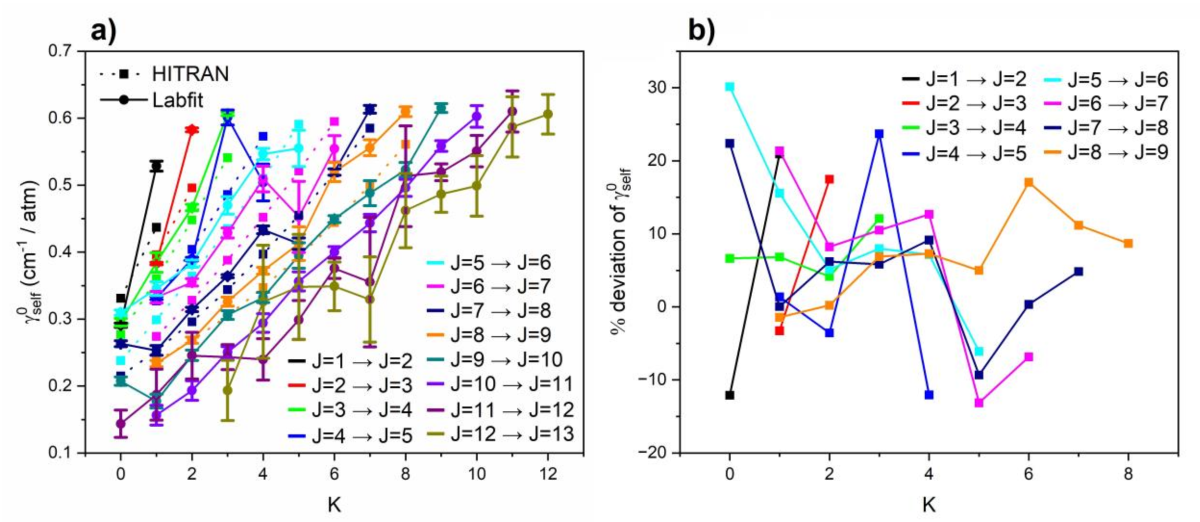

Figure S20. Plots of (a) self-broadened halfwidth, γ_{self}^{0}, and (b) percentage deviations from HITRAN of γ_{self}^{0} plotted against K for each J value of the $\nu_2(a) \leftarrow GS(s)$ R branch. The Labfit values are included with uncertainties of 3σ. For J" > 8, HITRAN values for the self-broadened halfwidth were all set to 0.5, so percentage deviations have not been calculated for these cases.

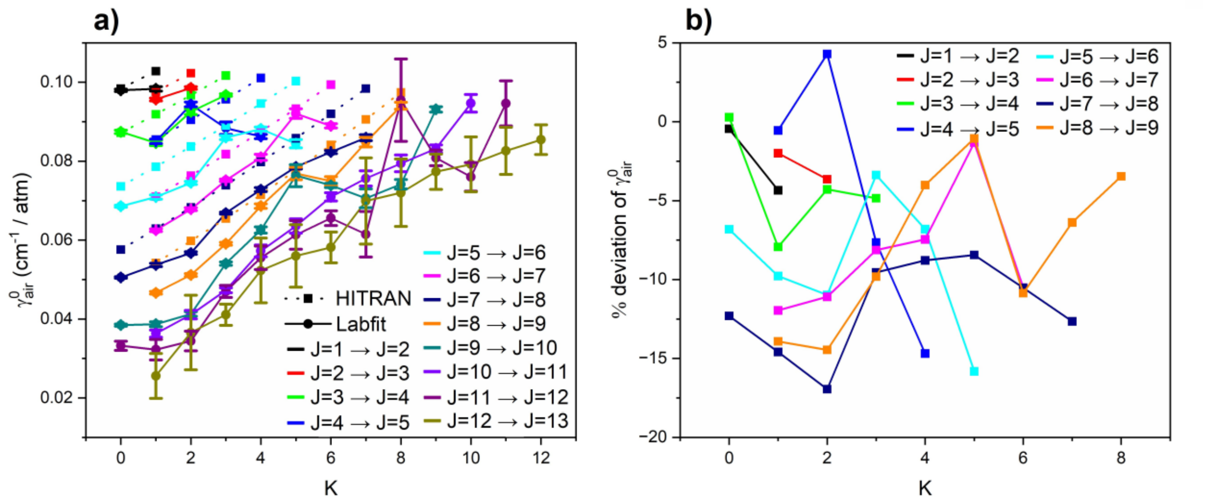

Figure S21. Plots of (a) air-broadened halfwidth, γ^0_{air}, and (b) percentage deviations from HITRAN of γ^0_{air} plotted against K for each J value of the $\nu_2(a) \leftarrow GS(s)$ R branch. The Labfit values are included with uncertainties of 3σ. For J" > 8, HITRAN values for the air-broadened halfwidth were set to the same value as their corresponding K value at J" = 8 (with values of K > 8 set to the value for K = 8), so percentage deviations have not been calculated for these cases.

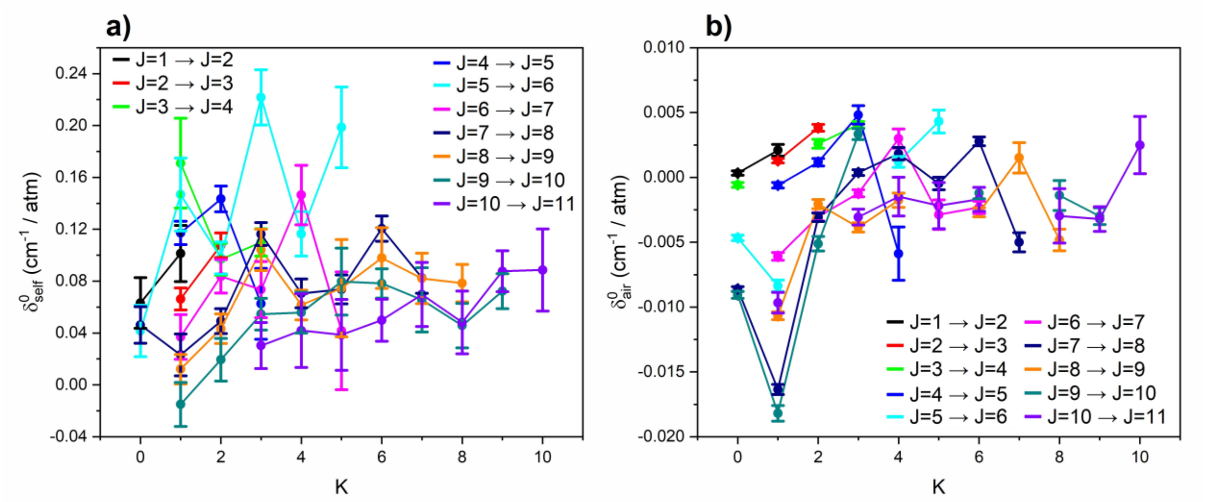

Figure S22. Plots of (a) self-pressure-induced shifts, δ^0_{self}, and (b) air-pressure-induced shifts, δ^0_{air}, against K for each J value of the $\nu_2(a) \leftarrow GS(s)$ R branch. Measured values are plotted with uncertainties of 3σ. The HITRAN 2020 database does not include values for these parameters.

S1.6 $\nu_2(s) \leftarrow GS(a)$ R branch plots

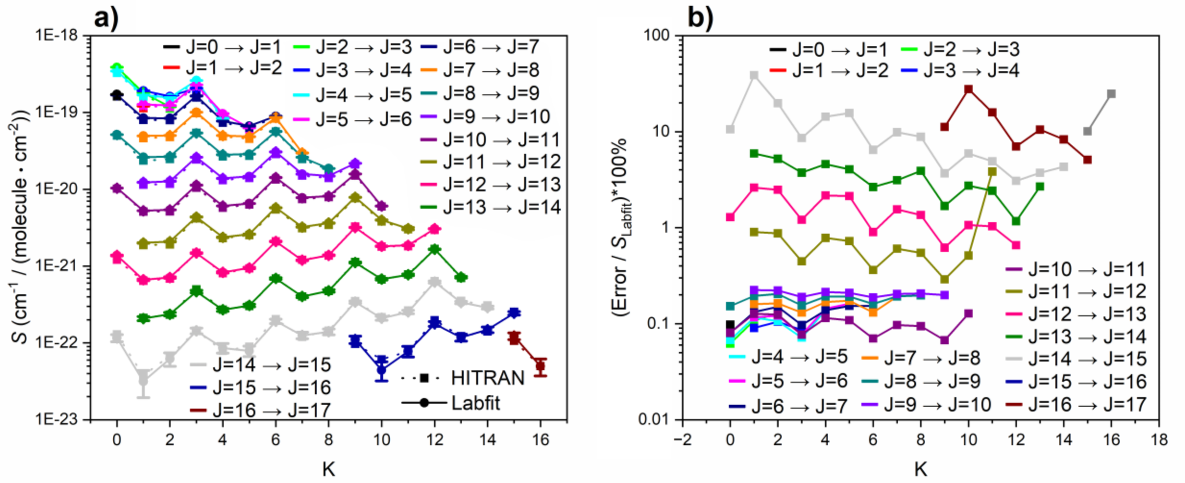

Figure S23. Plots of (a) spectral line intensity S, with Labfit value uncertainties of 3σ, and (b) 3σ uncertainty divided by Labfit line intensity S_{Labfit} plotted against K for each J value of the NH_3 $\nu_2(s) \leftarrow GS(a)$ R branch.

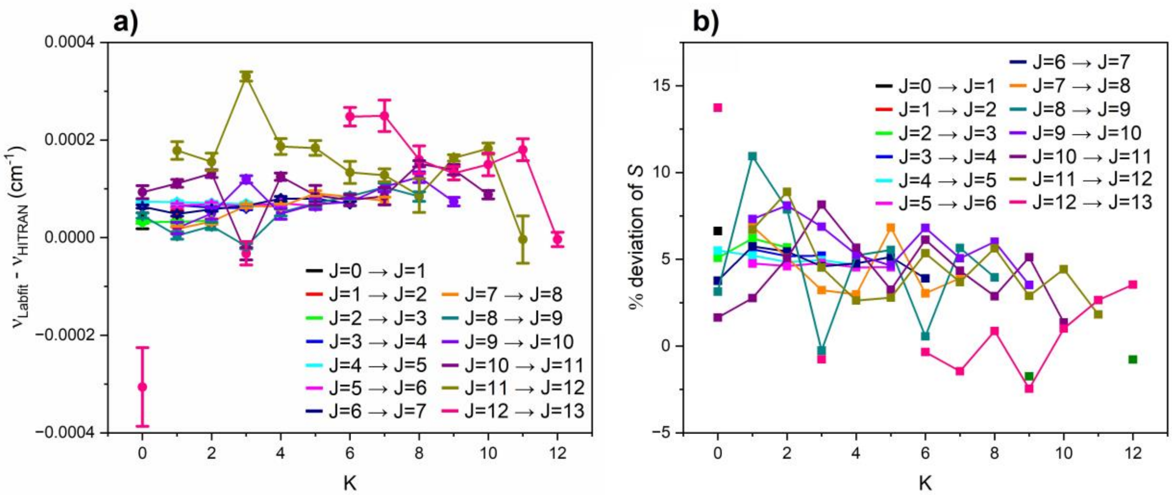

Figure S24. (a) Differences between the measured line positions and those from HITRAN 2020 for the NH_3 $\nu_2(s) \leftarrow GS(a)$ R branch lines, and (b) percentage deviations in intensity between the measured line intensities and those from HITRAN 2020 for the NH_3 $\nu_2(s) \leftarrow GS(a)$ R branch lines. For both cases, only lines with line intensity > 1 x 10^{-21} cm^{-1} / (molecule cm^{-2}) are plotted, and the error bars are 3σ.

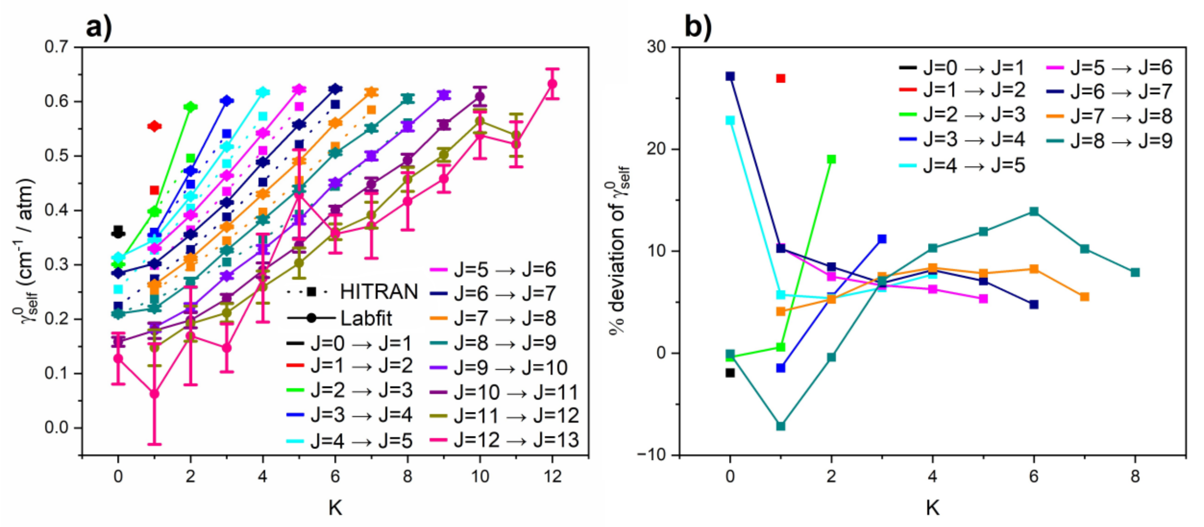

Figure S25. Plots of (a) self-broadened halfwidth, γ^0_{self}, and (b) percentage deviations from HITRAN of γ^0_{self} plotted against K for each J value of the $\nu_2(s) \leftarrow GS(a)$ R branch. The Labfit values are included with uncertainties of 3σ. For J" > 8, HITRAN values for the self-broadened halfwidth were all set to 0.5, so percentage deviations have not been calculated for these cases.

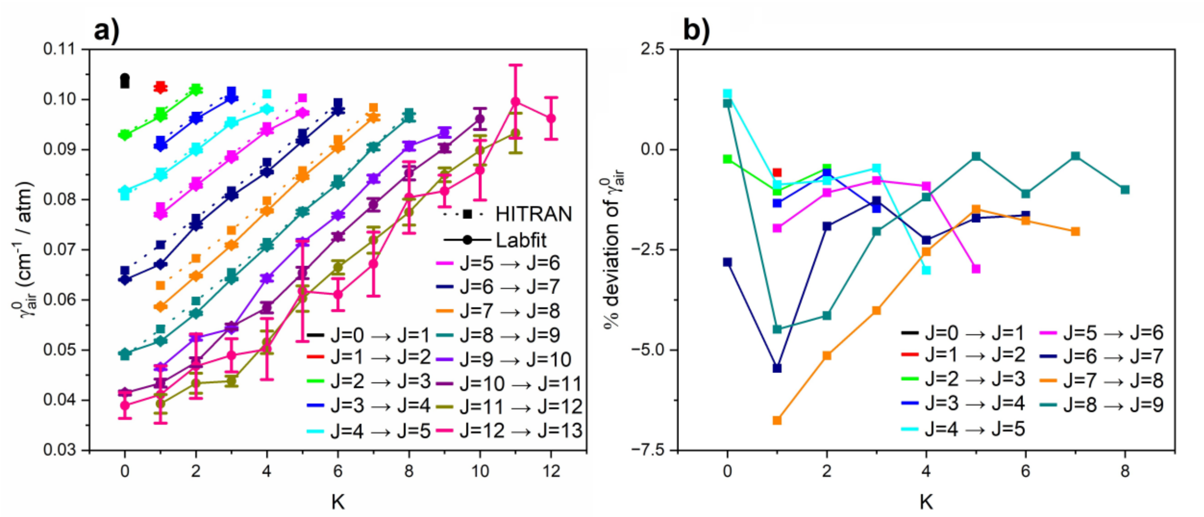

Figure S26. Plots of (a) air-broadened halfwidth, γ^0_{air}, and (b) percentage deviations from HITRAN of γ^0_{air} plotted against K for each J value of the $\nu_2(s) \leftarrow GS(a)$ R branch. The Labfit values are included with uncertainties of 3σ. For J" > 8, HITRAN values for the air-broadened halfwidth were set to the same value as their corresponding K value at J" = 8 (with values of K > 8 set to the value for K = 8), so percentage deviations have not been calculated for these cases.

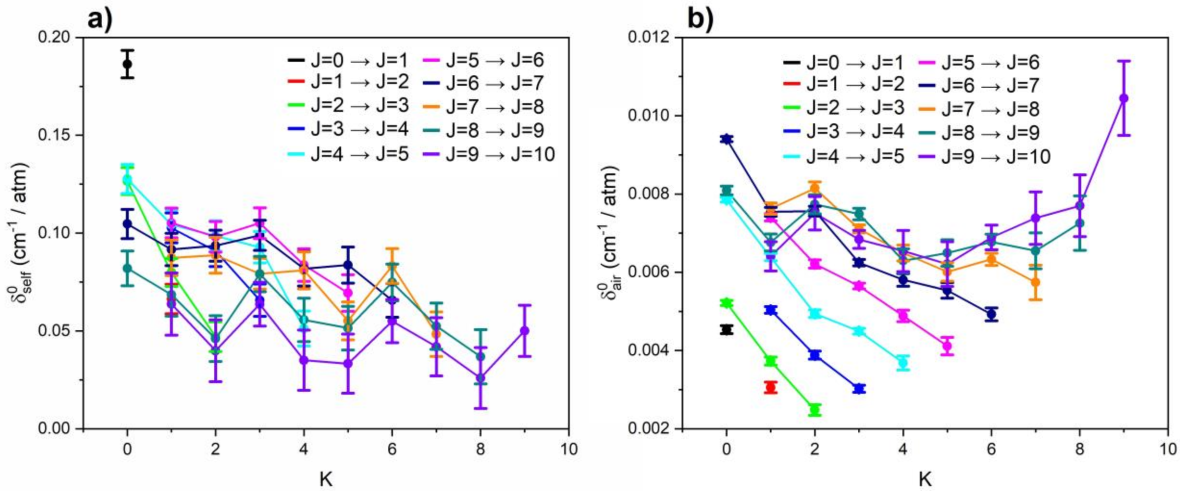

Figure S27. Plots of (a) self-pressure-induced shifts, δ^0_{self}, and (b) air-pressure-induced shifts, δ^0_{air}, against K for each J value of the $\nu_2(s) \leftarrow GS(a)$ R branch. Measured values are plotted with uncertainties of 3σ. The HITRAN 2020 database does not include values for these parameters.

S1.7 $\nu_2(a) \leftarrow GS(s)$ $^{15}NH_3$ Q branch plots

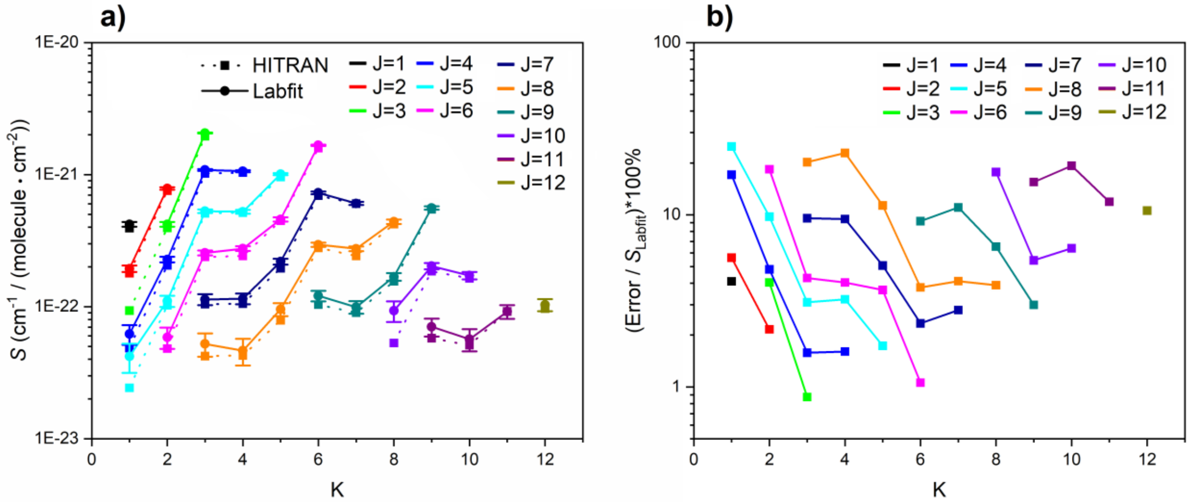

Figure S28. Plots of (a) spectral line intensity S, with Labfit value uncertainties of 3σ, and (b) 3σ uncertainty divided by Labfit line intensity S_{Labfit} plotted against K for each J value of the $^{15}NH_3$ $\nu_2(a) \leftarrow GS(s)$ Q branch.

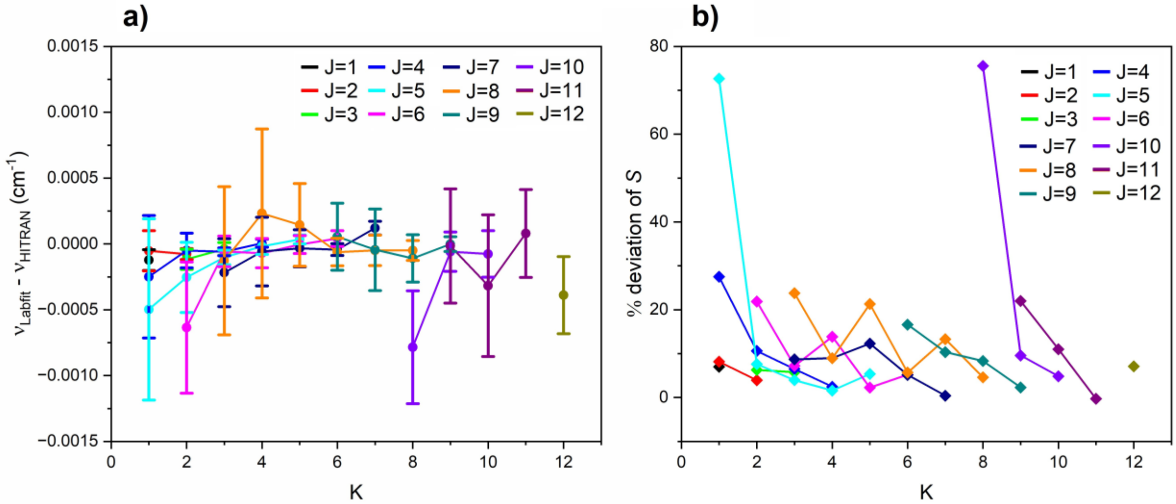

Figure S29. (a) Differences between the measured line positions and those from HITRAN 2020 for the $^{15}NH_3$ $\nu_2(a) \leftarrow GS(s)$ Q branch lines, and (b) percentage deviations in intensity between the measured line intensities and those from HITRAN 2020 for the $^{15}NH_3$ $\nu_2(a) \leftarrow GS(s)$ Q branch lines. For both cases, the error bars are 3σ.

S1.8 $\nu_2(s) \leftarrow GS(a)$ $^{15}NH_3$ Q branch plots

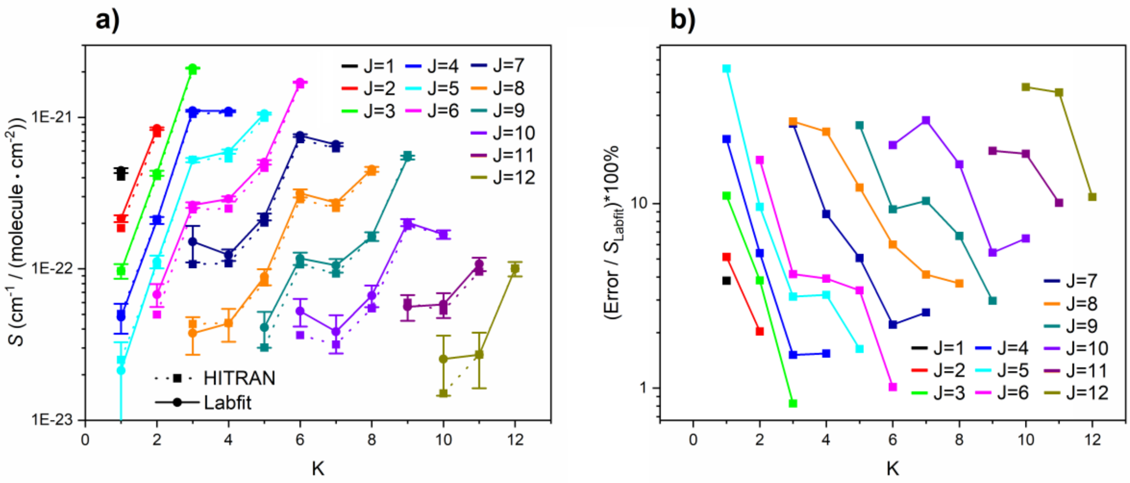

Figure S30. Plots of (a) spectral line intensity S, with Labfit value uncertainties of 3σ, and (b) 3σ uncertainty divided by Labfit line intensity S_{Labfit} plotted against K for each J value of the $^{15}NH_3$ $\nu_2(s) \leftarrow GS(a)$ Q branch.

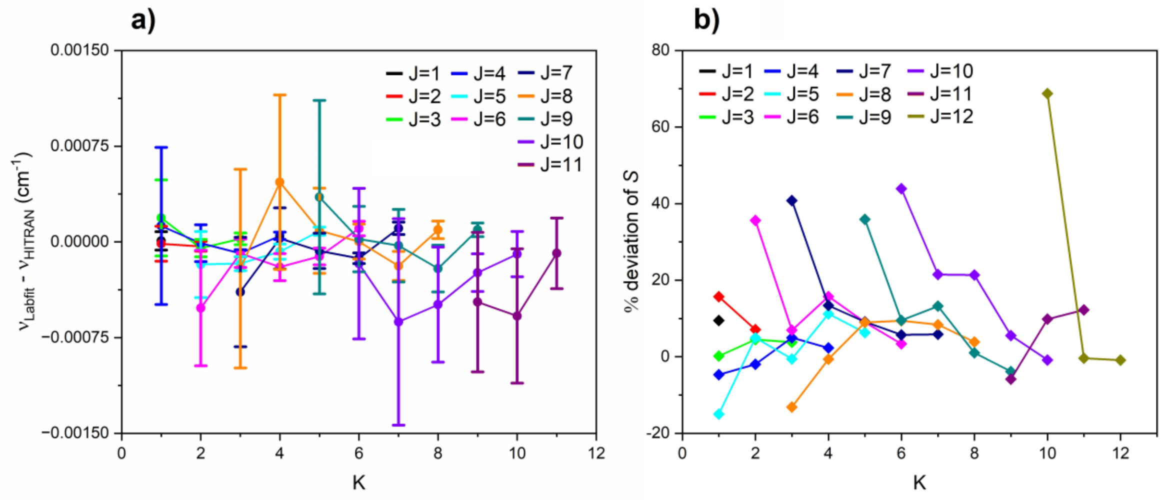

Figure S31. (a) Differences between the measured line positions and those from HITRAN 2020 for the $^{15}NH_3$ $\nu_2(s) \leftarrow GS(a)$ Q branch lines, and (b) percentage deviations in intensity between the measured line intensities and those from HITRAN 2020 for the $^{15}NH_3$ $\nu_2(s) \leftarrow GS(a)$ Q branch lines. For both cases, the error bars are 3σ.

S1.9 $2\nu_2(a) \leftarrow \nu_2(s)$ Q branch plots

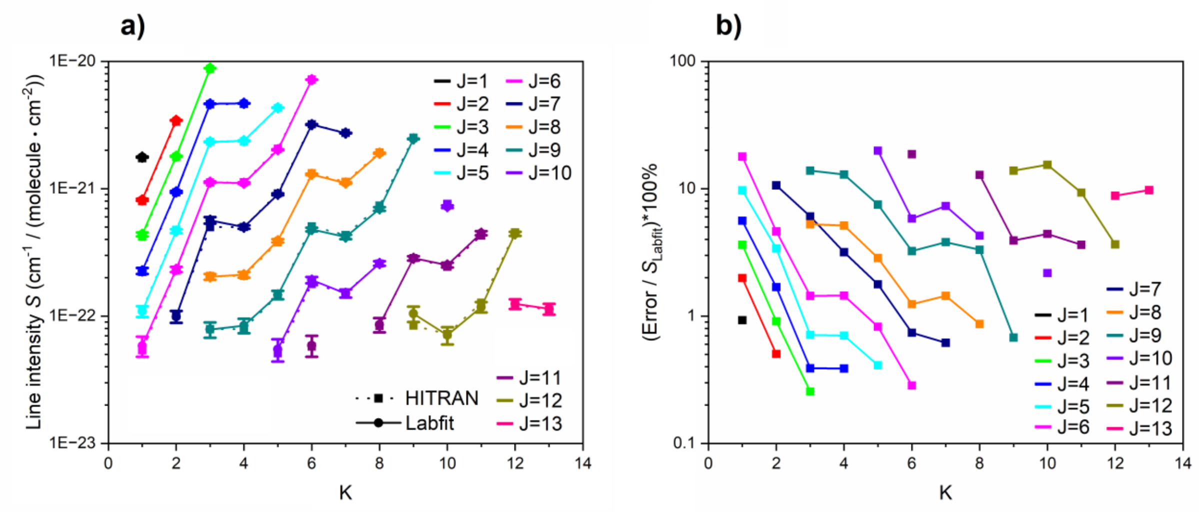

Figure S32 Plots of (a) spectral line intensity S, with Labfit value uncertainties of 3σ (b) 3σ uncertainty divided by Labfit line intensity S_{Labfit} plotted against K for each J value of the NH_3 $2\nu_2(a) \leftarrow \nu_2(s)$ Q branch.

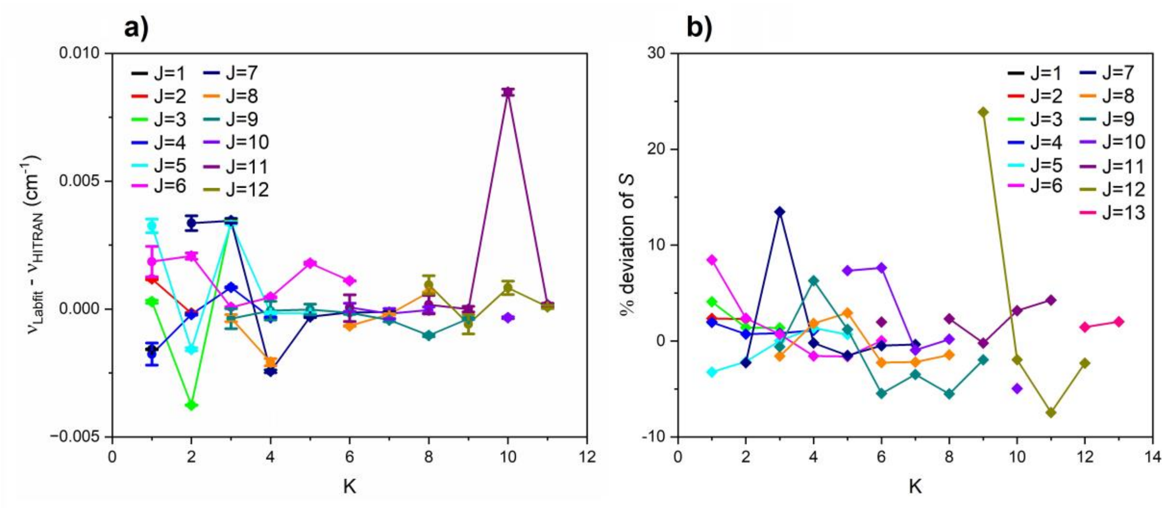

Figure S33. (a) Differences between the measured line positions and those from HITRAN 2020 for the NH_3 $2\nu_2(a) \leftarrow \nu_2(s)$ Q branch lines, and (b) percentage deviations in intensity between the measured line intensities and those from HITRAN 2020 for the NH_3 $2\nu_2(a) \leftarrow \nu_2(s)$ Q branch lines. For both cases, the error bars are 3σ.

S2 Line parameter lists

Table S1. Measured parameters at 296 K for lines (labelled ${}^{\Delta K}\Delta J(J'', K'')_{i''}$) with spectral intensity < 1 x 10^{-21} cm^{-1} / (molecule cm^{-2}) for the transition $\nu_2(s) \leftarrow GS(a)$. The numbers in parentheses are 1σ uncertainties in the units of the last digit listed. Missing entries indicate a lack of convergence for a given parameter, which was set to zero in the final solution. An asterisk (*) indicates that the line parameter was fixed to its value in HITRAN 2020.

Line	ν_0 cm^{-1}	$S \times 10^{21}$ cm^{-1} / (mol. cm^{-2}))	γ^0_{air} cm^{-1}/atm	γ^0_{self} cm^{-1}/atm	δ^0_{air} cm^{-1}/atm	δ^0_{self} cm^{-1}/atm
${}^{Q}P(12,10)_a$	685.278476(21)	0.7299(63)	0.0906*	0.500*		
${}^{Q}P(13,6)_a$	686.391684(41)	0.3612(60)	0.0841*	0.500*		
${}^{Q}P(13,5)_a$	688.841003(79)	0.1876(59)	0.0777*	0.500*		
${}^{Q}P(13,4)_a$	690.766549(86)	0.1706(59)	0.0715*	0.500*		
${}^{Q}P(13,3)_a$	692.231411(58)	0.2569(60)	0.0655*	0.500*		
${}^{Q}P(13,2)_a$	693.229939(110)	0.1335(59)	0.0598*	0.500*		
${}^{Q}P(13,1)_a$	693.810004(164)	0.0900(58)	0.0542*	0.500*		
${}^{Q}P(12,8)_a$	695.790587(22)	0.6765(63)	0.0974*	0.500*		
${}^{Q}P(12,7)_a$	699.724260(23)	0.6624(63)	0.0906*	0.500*		
${}^{Q}P(12,5)_a$	705.531578(29)	0.5330(62)	0.0777*	0.500*		
${}^{Q}P(12,4)_a$	707.566322(31)	0.4921(61)	0.0715*	0.500*		
${}^{Q}P(12,3)_a$	709.088776(16)	0.9498(64)	0.0655*	0.500*		
${}^{Q}P(12,2)_a$	710.165449(36)	0.4260(61)	0.0598*	0.500*		
${}^{Q}P(12,1)_a$	710.787047(32)	0.4706(61)	0.0542*	0.500*		
${}^{Q}P(12,0)_a$	711.021589(19)	0.8326(63)	0.0488*	0.500*		
${}^{Q}Q(19,19)_a$	879.320813(750)	0.0164(39)	0.0906*	0.500*		
${}^{Q}Q(18,18)_a$	885.210252(74)	0.1453(39)	0.0906*	0.500*		
${}^{Q}Q(17,17)_a$	890.690236(48)	0.2260(39)	0.0906*	0.500*		
${}^{Q}Q(19,18)_a$	892.858407(455)	0.0246(39)	0.0906*	0.500*		
${}^{Q}Q(16,16)_a$	895.773561(20)	0.5852(61)	0.0900(63)	0.631(37)		
${}^{Q}Q(18,17)_a$	897.605647(304)	0.0366(39)	0.0906*	0.500*		
${}^{Q}Q(17,16)_a$	902.014116(93)	0.1077(36)	0.0906*	0.500*		
${}^{Q}Q(16,15)_a$	906.091976(19)	0.5501(38)	0.0906*	0.500*		
${}^{Q}Q(15,14)_a$	909.848121(15)	0.7091(39)	0.9060*	0.500*		
${}^{Q}Q(17,15)_a$	911.276057(90)	0.1120(36)	0.0906*	0.500*		
$Q(16,14)_a$	914.556284(70)	0.1438(36)	0.0906*	0.500*		
${}^{Q}Q(15,13)_a$	917.559271(29)	0.3493(37)	0.0906*	0.500*		
${}^{Q}Q(16,13)_a$	921.515400(146)	0.0694(36)	0.0906*	0.500*		
${}^{Q}Q(15,12)_a$	923.914070(26)	0.4007(38)	0.0906*	0.500*		
${}^{Q}Q(14,11)_a$	926.067820(21)	0.4789(56)	0.0906*	0.457(40)		
${}^{Q}Q(16,12)_a$	927.252432(132)	0.0782(37)	0.0906*	0.500*		
${}^{Q}Q(14,10)_a$	930.843124(38)	0.3360(61)	0.0906*	1.001(72)		
${}^{Q}Q(14,9)_a$	934.790753(32)	0.3127(54)	0.1044*	0.437(59)		
${}^{Q}Q(13,8)_a$	935.850507(26)	0.3582(53)	0.0974*	0.242(47)		
${}^{Q}Q(12,7)_a$	936.678546(13)	0.8410(39)	0.0906*	0.500*		
${}^{Q}Q(15,9)_a$	937.099720(173)	0.0596(36)	0.1044*	0.500*		
${}^{Q}Q(14,8)_a$	938.049200(122)	0.0865(37)	0.0974*	0.557*		
${}^{Q}Q(13,7)_a$	938.770722(44)	0.2306(55)	0.0906*	0.486(82)		
${}^{Q}Q(12,6)_a$	939.256456(11)	0.9892(40)	0.0841*	0.500*		
${}^{Q}Q(8,1)_a$	939.263650(16)	0.5850(37)	0.0629*	0.253*		
${}^{Q}Q(11,5)_a$	939.496240(11)	0.9810(40)	0.0777*	0.500*		
${}^{Q}Q(15,8)_a$	940.071383(335)	0.0318(36)	0.0974*	0.500*		
${}^{Q}Q(14,7)_a$	940.727137(181)	0.0569(36)	0.0906*	0.500*		
${}^{Q}Q(9,1)_a$	940.836079(41)	0.2495(37)	0.0542*	0.500*		
${}^{Q}Q(13,6)_a$	941.147791(38)	0.2592(54)	0.0841*	0.431(71)		
${}^{Q}Q(11,4)_a$	941.237766(19)	0.5387(38)	0.0715*	0.500*		
${}^{Q}Q(12,5)_a$	941.322418(36)	0.2877(37)	0.0777*	0.500*		
${}^{Q}Q(10,2)_a$	941.850922(29)	0.3508(37)	0.0598*	0.500*		
${}^{Q}Q(10,1)_a$	942.419259(124)	0.0832(36)	0.0542*	0.500*		
${}^{Q}Q(15,7)_a$	942.516156(617)	0.0192(37)	0.0906*	0.500*		
${}^{Q}Q(11,3)_a$	942.565813(19)	0.5379(38)	0.0655*	0.500*		
${}^{Q}Q(12,4)_a$	942.938391(67)	0.1536(37)	0.0715*	0.500*		
${}^{Q}Q(11,2)_a$	943.450696(87)	0.1179(36)	0.0598*	0.500*		
${}^{Q}Q(11,1)_a$	943.976204(325)	0.0328(36)	0.0542*	0.500*		
${}^{Q}Q(12,3)_a$	944.114419(56)	0.1827(37)	0.0655*	0.500*		
${}^{Q}Q(13,4)_a$	944.547169(252)	0.0427(36)	0.0715*	0.500*		
${}^{Q}Q(14,5)_a$	944.662057(550)	0.0215(37)	0.0777*	0.500*		

${}^{Q}Q(12,2)_a$	944.991869(332)	0.0323(36)	0.0598*	0.500*		
${}^{Q}Q(13,3)_a$	945.724784(329)	0.0363(38)	0.0655*	0.500*		
${}^{Q}R(13,13)_a$	1189.773945(19)	0.6953(43)	0.0906*	0.500*		
${}^{Q}R(12,5)_a$	1195.536101(14)	0.9477(67)	0.0617(33)	0.433(27)		
${}^{Q}R(12,4)_a$	1196.718643(15)	0.8296(60)	0.0502(20)	0.276(27)		
${}^{Q}R(12,2)_a$	1198.208516(16)	0.7107(59)	0.0459(21)	0.170(30)	0.00855(204)	
${}^{Q}R(12,1)_a$	1198.529511(17)	0.6648(58)	0.0410(19)	0.063(31)		
${}^{Q}R(13,11)_a$	1200.541153(17)	0.7744(43)	0.0906*	0.500*		
${}^{Q}R(13,10)_a$	1204.473634(19)	0.6865(43)	0.0906*	0.500*		
${}^{Q}R(14,14)_a$	1205.875011(45)	0.2887(41)	0.0906*	0.500*		
${}^{Q}R(13,8)_a$	1210.282968(27)	0.4800(42)	0.0974*	0.500*		
${}^{Q}R(14,13)_a$	1212.355607(39)	0.3360(42)	0.0906*	0.500*		
${}^{Q}R(13,7)_a$	1212.396026(33)	0.4021(42)	0.0906*	0.500*		
${}^{Q}R(13,6)_a$	1214.096699(18)	0.6914(61)	0.0593(31)	0.361(34)	0.01161(302)	
${}^{Q}R(13,5)_a$	1215.447207(43)	0.3076(41)	0.0777*	0.500*		
${}^{Q}R(13,4)_a$	1216.495178(49)	0.2701(41)	0.0715*	0.500*		
${}^{Q}R(13,3)_a$	1217.265878(26)	0.5044(42)	0.0655*	0.500*		
${}^{Q}R(14,12)_a$	1217.606827(22)	0.6093(42)	0.0906*	0.500*		
${}^{Q}R(13,2)_a$	1217.814255(55)	0.2368(41)	0.0598*	0.500*		
${}^{Q}R(13,1)_a$	1218.038981(63)	0.2075(41)	0.0542*	0.500*		
${}^{Q}R(15,15)_a$	1221.627784(54)	0.2436(41)	0.0906*	0.500*		
${}^{Q}R(14,11)_a$	1221.869262(52)	0.2531(41)	0.0906*	0.500*		
${}^{Q}R(14,10)_a$	1225.334573(63)	0.2093(41)	0.0906*	0.500*		
${}^{Q}R(14,9)_a$	1228.154360(39)	0.3406(42)	0.1044*	0.500*		
${}^{Q}R(15,14)_a$	1228.679162(88)	0.1488(41)	0.0906*	0.500*		
${}^{Q}R(14,8)_a$	1230.447206(95)	0.1397(41)	0.0974*	0.500*		
${}^{Q}R(14,7)_a$	1232.305019(105)	0.1255(41)	0.0906*	0.500*		
${}^{Q}R(14,6)_a$	1233.799414(69)	0.1918(41)	0.0841*	0.500*		
${}^{Q}R(15,13)_a$	1234.367529(112)	0.1177(41)	0.0906*	0.500*		
${}^{Q}R(14,5)_a$	1234.986124(169)	0.0787(41)	0.0777*	0.500*		
${}^{Q}R(14,4)_a$	1235.907050(154)	0.0860(41)	0.0715*	0.500*		
${}^{Q}R(14,3)_a$	1236.607126(92)	0.1438(41)	0.0655*	0.500*		
${}^{Q}R(14,1)_a$	1236.945559(435)	0.0316(41)	0.0542*	0.500*		
${}^{Q}R(16,16)_a$	1237.022292(270)	0.0496(41)	0.0906*	0.500*		
${}^{Q}R(14,2)_a$	1237.063637(214)	0.0620(41)	0.0598*	0.500*		
${}^{Q}R(14,0)_a$	1237.462351(114)	0.1158(41)	0.0488*	0.500*		
${}^{Q}R(15,12)_a$	1238.964500(75)	0.1770(41)	0.0906*	0.500*		
${}^{Q}R(15,11)_a$	1242.689426(171)	0.0778(41)	0.0906*	0.500*		
${}^{Q}R(16,15)_a$	1244.676056(108)	0.1228(41)	0.0906*	0.500*		
${}^{Q}R(15,10)_a$	1245.714620(302)	0.0444(41)	0.0906*	0.500*		
${}^{Q}R(15,9)_a$	1248.173570(120)	0.1105(41)	0.1044*	0.500*		

Table S2. Measured parameters at 296 K for lines (labelled ${}^{\Delta K}\Delta J(J'',K'')_{i''}$) with spectral intensity < 1 x 10^{-21} cm^{-1} / (molecule cm^{-2}) for the transition $\nu_2(a) \leftarrow GS(s)$. The numbers in parentheses are 1σ uncertainties in the units of the last digit listed. Missing entries indicate a lack of convergence for a given parameter, which was set to zero in the final solution. An asterisk (*) indicates that the line parameter was fixed to its value in HITRAN 2020.

Line	$\boldsymbol{\nu_0}$ cm^{-1}	$\boldsymbol{S \times 10^{21}}$ cm^{-1} / (mol. cm^{-2}))	$\boldsymbol{\gamma^0_{air}}$ cm^{-1}/atm	$\boldsymbol{\gamma^0_{self}}$ cm^{-1}/atm	$\boldsymbol{\delta^0_{air}}$ cm^{-1}/atm	$\boldsymbol{\delta^0_{self}}$ cm^{-1}/atm
${}^{Q}P(14,9)_s$	685.037670(82)	0.1789(59)	0.1044*	0.500*		
${}^{Q}P(14,8)_s$	686.313345(175)	0.0839(59)	0.0974*	0.500*		
${}^{Q}P(14,7)_s$	687.471330(171)	0.0859(59)	0.0906*	0.500*		
${}^{Q}P(14,6)_s$	688.497165(107)	0.1369(59)	0.0841*	0.500*		
${}^{Q}P(14,5)_s$	689.377110(229)	0.0649(59)	0.0777*	0.500*		
${}^{Q}P(14,4)_s$	690.101063(501)	0.0299(58)	0.0715*	0.500*		
${}^{Q}P(14,3)_s$	690.656987(224)	0.0667(58)	0.0655*	0.500*		
${}^{Q}P(14,1)_s$	691.336136(359)	0.0419(58)	0.0542*	0.500*		
${}^{Q}P(13,12)_s$	700.774461(29)	0.5143(62)	0.0906*	0.500*		
${}^{Q}P(13,11)_s$	701.959394(48)	0.3090(60)	0.0906*	0.500*		
${}^{Q}P(13,10)_s$	703.193972(53)	0.2806(60)	0.0906*	0.500*		
${}^{Q}P(13,9)_s$	704.413743(27)	0.5529(62)	0.1044*	0.500*		
${}^{Q}P(13,8)_s$	705.573115(65)	0.2303(60)	0.0974*	0.500*		
${}^{Q}P(13,7)_s$	706.640189(69)	0.2157(60)	0.0906*	0.500*		
${}^{Q}P(13,6)_s$	707.592538(40)	0.3727(61)	0.0841*	0.500*		

$^{Q}P(13,5)_s$	708.414835(81)	0.1828(59)	0.0777*	0.500*	
$^{Q}P(13,4)_s$	709.097594(95)	0.1571(59)	0.0715*	0.500*	
$^{Q}P(13,3)_s$	709.637621(54)	0.2762(60)	0.0655*	0.500*	
$^{Q}P(13,2)_s$	710.049153(113)	0.1317(59)	0.0598*	0.500*	
$^{Q}P(13,1)_s$	710.262354(101)	0.1481(59)	0.0542*	0.500*	
$^{Q}P(13,0)_s$	710.338772(59)	0.2535(60)	0.0488*	0.500*	
$^{Q}P(12,11)_s$	721.970707(26)	0.5843(62)	0.0906*	0.500*	
$^{Q}P(12,10)_s$	723.002427(21)	0.7540(63)	0.0906*	0.500*	
$^{Q}P(12,8)_s$	725.092294(22)	0.7117(63)	0.0974*	0.500*	
$^{Q}P(12,7)_s$	726.057353(24)	0.6463(63)	0.0906*	0.500*	
$^{Q}P(12,5)_s$	727.688940(29)	0.5293(62)	0.0777*	0.500*	
$^{Q}P(12,4)_s$	728.323004(32)	0.4727(61)	0.0715*	0.500*	
$^{Q}P(12,3)_s$	728.812912(16)	0.9608(64)	0.0655*	0.500*	
$^{Q}P(12,2)_s$	729.202925(33)	0.4634(61)	0.0598*	0.500*	
$^{Q}P(12,1)_s$	729.411246(35)	0.4395(61)	0.0542*	0.500*	
$^{Q}Q(19,18)_s$	943.678622(386)	0.0281(36)	0.0906*	0.500*	
$^{Q}Q(19,19)_s$	943.764732(296)	0.0360(36)	0.0906*	0.500*	
$^{Q}Q(18,18)_s$	946.067902(74)	0.1393(37)	0.0906*	0.500*	
$^{Q}Q(18,17)_s$	946.088322(266)	0.0398(36)	0.0906*	0.500*	
$^{Q}Q(17,17)_s$	948.285305(50)	0.2058(37)	0.0906*	0.500*	
$^{Q}Q(17,16)_s$	948.387175(102)	0.1006(37)	0.0906*	0.500*	
$^{Q}Q(17,15)_s$	948.919060(122)	0.0903(38)	0.0906*	0.652*	
$^{Q}Q(17,14)_s$	949.716299(512)	0.0230(36)	0.0906*	0.500*	
$^{Q}Q(16,16)_s$	950.408606(19)	0.5531(38)	0.0906*	0.500*	
$^{Q}Q(16,15)_s$	950.570501(19)	0.5377(38)	0.0906*	0.500*	
$^{Q}Q(16,14)_s$	951.093385(86)	0.1203(37)	0.0906*	0.500*	
$^{Q}Q(16,13)_s$	951.835604(139)	0.0748(37)	0.0906*	0.500*	
$^{Q}Q(15,14)_s$	952.635253(16)	0.6784(39)	0.0906*	0.500*	
$^{Q}Q(16,12)_s$	952.696460(120)	0.0866(37)	0.0906*	0.500*	
$^{Q}Q(15,13)_s$	953.139399(29)	0.3550(37)	0.0906*	0.500*	
$^{Q}Q(16,11)_s$	953.605647(371)	0.0288(36)	0.0906*	0.500*	
$^{Q}Q(15,12)_s$	953.822345(28)	0.3767(38)	0.0906*	0.500*	
$^{Q}Q(15,11)_s$	954.598273(115)	0.0901(37)	0.0906*	0.500*	
$^{Q}Q(15,10)_s$	955.405641(177)	0.0585(36)	0.0906*	0.500*	
$^{Q}Q(14,11)_s$	955.676766(22)	0.4692(38)	0.0906*	0.500*	
$^{Q}Q(15,9)_s$	956.202487(129)	0.0809(37)	0.1044*	0.500*	
$^{Q}Q(14,10)_s$	956.367548(37)	0.2774(37)	0.0906*	0.500*	
$^{Q}Q(14,9)_s$	957.075981(34)	0.3075(37)	0.1044*	0.500*	
$^{Q}Q(14,8)_s$	957.765390(129)	0.0804(37)	0.0974*	0.500*	
$^{Q}Q(14,7)_s$	958.409008(150)	0.0689(37)	0.0906*	0.500*	
$^{Q}Q(13,8)_s$	958.617636(28)	0.3753(38)	0.0974*	0.500*	
$^{Q}Q(13,7)_s$	959.202964(111)	0.3249(66)	0.0906*	0.500*	
$^{Q}Q(13,6)_s$	959.739335(39)	0.2681(37)	0.0841*	0.500*	
$^{Q}Q(12,7)_s$	960.032457(13)	0.8120(58)	0.0763(50)	0.406(25)	
$^{Q}Q(13,5)_s$	960.211321(132)	0.0785(37)	0.0777*	0.500*	
$^{Q}Q(12,6)_s$	960.518195(11)	0.9160(54)	0.0595(24)	0.307(20)	
$^{Q}Q(13,4)_s$	960.607586(191)	0.0545(37)	0.0715*	0.500*	
$^{Q}Q(12,5)_s$	960.952024(47)	0.2801(41)	0.0777*	0.500*	
$^{Q}Q(12,3)_s$	961.666567(62)	0.1675(37)	0.0655*	0.500*	
$^{Q}Q(11,5)_s$	961.713336(11)	0.9162(55)	0.0610(26)	0.313(20)	
$^{Q}Q(12,2)_s$	961.857774(193)	0.0541(36)	0.0598*	0.500*	
$^{Q}Q(11,4)_s$	962.049643(20)	0.5365(38)	0.0715*	0.500*	
$^{Q}Q(11,3)_s$	962.279940(20)	0.5374(38)	0.0655*	0.500*	
$^{Q}Q(11,2)_s$	962.537728(101)	0.1024(37)	0.0598*	0.500*	
$^{Q}Q(11,1)_s$	962.648872(406)	0.0272(37)	0.0542*	0.500*	
$^{Q}Q(10,2)_s$	963.229760(30)	0.3501(38)	0.0598*	0.500*	
$^{Q}Q(10,1)_s$	963.336343(103)	0.1022(37)	0.0542*	0.500*	
$^{Q}Q(9,2)_s$	963.924234(10)	0.9169(54)	0.0514(21)	0.216(19)	
$^{Q}Q(9,1)_s$	964.022560(40)	0.2297(54)	0.0579(119)	0.233(75)	
$^{Q}Q(8,1)_s$	964.698481(16)	0.6033(54)	0.0429(28)	0.271(29)	
$^{Q}R(12,5)_s$	1212.748221(14)	0.8959(61)	0.0551(23)	0.350(26)	
$^{Q}R(12,4)_s$	1212.830128(15)	0.8234(61)	0.0502(22)	0.328(28)	
$^{Q}R(12,1)_s$	1213.007932(55)	0.6745(231)	0.0252(18)	0.127(49)	
$^{Q}R(12,2)_s$	1213.011271(54)	0.6817(231)	0.0388(32)	0.122(49)	
$^{Q}R(13,8)_s$	1230.069687(29)	0.4629(42)	0.0974*	0.500*	
$^{Q}R(13,10)_s$	1230.095209(21)	0.6288(43)	0.0906*	0.500*	
$^{Q}R(13,7)_s$	1230.139965(34)	0.3853(42)	0.0906*	0.500*	
$^{Q}R(13,6)_s$	1230.232290(20)	0.6656(43)	0.0841*	0.500*	
$^{Q}R(13,11)_s$	1230.267009(19)	0.7242(43)	0.0906*	0.500*	
$^{Q}R(13,5)_s$	1230.330171(46)	0.2899(42)	0.0777*	0.500*	
$^{Q}R(13,4)_s$	1230.421654(49)	0.2681(41)	0.0715*	0.500*	

$^{Q}R(13,3)_s$	1230.541698(26)	0.5039(42)	0.0655*	0.500*		
$^{Q}R(13,1)_s$	1230.613063(70)	0.2172(50)	0.0542*	0.500*		
$^{Q}R(13,0)_s$	1230.622768(141)	0.5383(648)	0.0488*	0.500*		
$^{Q}R(13,2)_s$	1230.669759(58)	0.2269(41)	0.0598*	0.500*		
$^{Q}R(13,13)_s$	1231.240820(21)	0.6468(43)	0.0906*	0.500*		
$^{Q}R(14,10)_s$	1247.322190(62)	0.2208(42)	0.0906*	0.500*		
$^{Q}R(14,9)_s$	1247.330459(41)	0.3319(42)	0.1044*	0.500*		
$^{Q}R(14,8)_s$	1247.396672(104)	0.1277(41)	0.0974*	0.500*		
$^{Q}R(14,11)_s$	1247.408967(53)	0.2501(42)	0.0906*	0.500*		
$^{Q}R(14,7)_s$	1247.494458(115)	0.1163(41)	0.0906*	0.500*		
$^{Q}R(14,6)_s$	1247.604573(70)	0.1914(41)	0.0841*	0.500*		
$^{Q}R(14,12)_s$	1247.642566(23)	0.5996(43)	0.0906*	0.500*		
$^{Q}R(14,5)_s$	1247.713771(166)	0.0807(41)	0.0777*	0.500*		
$^{Q}R(14,4)_s$	1247.811753(171)	0.0778(41)	0.0715*	0.500*		
$^{Q}R(14,3)_s$	1247.831959(98)	0.1356(41)	0.0655*	0.500*		
$^{Q}R(14,1)_s$	1248.012604(220)	0.0613(41)	0.0542*	0.500*		
$^{Q}R(14,13)_s$	1248.094528(39)	0.3447(42)	0.0906*	0.500*		
$^{Q}R(14,2)_s$	1248.373562(269)	0.0499(41)	0.0598*	0.500*		
$^{Q}R(14,14)_s$	1248.864753(44)	0.3049(42)	0.0906*	0.500*		

Table S3. Measured parameters at 296 K for lines (labelled $^{\Delta K}\Delta J(J'',K'')_{i''}$) of the transition $2\nu_2(s) \leftarrow \nu_2(a)$. The numbers in parentheses are 1σ uncertainties in the units of the last digit listed. Missing entries indicate a lack of convergence for a given parameter, which was set to zero in the final solution. An asterisk (*) indicates that the line parameter was fixed to its value in HITRAN 2020.

Line	$\boldsymbol{\nu_0}$ cm-1	$\boldsymbol{S} \times 10^{21}$ cm-1 / (mol. cm-2))	$\boldsymbol{\gamma^0_{air}}$ cm-1/atm	$\boldsymbol{\gamma^0_{self}}$ cm-1/atm	$\boldsymbol{\delta^0_{air}}$ cm-1/atm	$\boldsymbol{\delta^0_{self}}$ cm-1/atm
$^{Q}R(2,2)_a$	690.173890(8)	3.1875(161)	0.0944(19)	0.233(13)		
$^{Q}R(2,1)_a$	691.763015(11)	4.6734(99)	0.0926(13)	0.204(6)	0.00629(126)	0.049(14)
$^{Q}R(2,0)_a$	692.306143(6)	10.3130(164)	0.0882(6)	0.227(3)	0.00618(54)	0.072(8)
$^{Q}R(3,3)_a$	709.651451(10)	5.2148(103)	0.0911(11)	0.207(6)		-0.072(12)
$^{Q}R(3,2)_a$	712.319915(4)	4.1133(96)	0.0932(15)	0.215(7)		
$^{Q}R(3,1)_a$	713.995371(4)	4.9232(101)	0.0815(10)	0.239(6)		
$^{Q}R(4,4)_a$	728.570494(15)	1.9693(223)	0.0963(64)	0.219(21)		
$^{Q}R(4,3)_a$	732.295462(9)	6.3671(112)	0.0902(9)	0.244(5)		-0.055(11)
$^{Q}R(4,2)_a$	735.138391(4)	3.8386(95)	0.0864(14)	0.215(8)		
$^{Q}R(4,1)_a$	736.908112(4)	4.2302(97)	0.0777(11)	0.247(7)		
$^{Q}R(4,0)_a$	737.509252(3)	8.6073(136)	0.0763(5)	0.213(4)	0.00393(52)	
$^{Q}R(5,5)_a$	746.869772(11)	1.3598(87)	0.0960(46)	0.216(19)		
$^{Q}R(5,4)_a$	751.612766(7)	2.1529(90)	0.0846(24)	0.263(13)		
$^{Q}R(5,3)_a$	755.627752(10)	5.2698(103)	0.0806(9)	0.251(6)		-0.084(13)
$^{Q}R(5,2)_a$	758.645742(5)	2.9403(92)	0.0778(16)	0.237(10)		
$^{Q}R(5,1)_a$	760.517687(5)	3.0937(92)	0.0780(15)	0.215(9)		
$^{Q}R(6,6)_a$	764.513488(9)	1.6906(90)	0.0978(38)	0.322(17)		
$^{Q}R(6,5)_a$	770.214125(11)	1.2690(87)	0.0811(39)	0.224(21)		
$^{Q}R(6,4)_a$	775.352469(9)	1.6204(89)	0.0744(27)	0.296(17)		
$^{Q}R(6,3)_a$	779.620739(5)	3.4984(94)	0.0731(14)	0.214(8)		
$^{Q}R(7,7)_a$	781.519319(34)	0.4774(63)	0.0984*	0.585*		
$^{Q}R(6,2)_a$	782.833930(8)	1.9143(89)	0.0736(22)	0.223(14)		
$^{Q}R(6,1)_a$	784.800063(8)	1.9269(88)	0.0611(17)	0.188(14)		
$^{Q}R(6,0)_a$	785.513727(4)	3.9972(95)	0.0629(9)	0.188(7)		
$^{Q}R(7,6)_a$	788.107551(11)	1.3470(88)	0.1025(63)	0.184(20)		
$^{Q}R(7,5)_a$	794.274559(19)	0.8579(64)	0.0858*	0.455*		
$^{Q}R(7,4)_a$	799.706225(16)	0.9516(64)	0.0798*	0.397*		
$^{Q}R(7,3)_a$	804.231273(8)	1.9763(89)	0.0625(17)	0.222(14)		
$^{Q}R(8,7)_a$	805.385251(45)	0.3530(62)	0.0906*	0.500*		
$^{Q}R(7,2)_a$	807.654074(14)	1.0579(88)	0.0636(38)	0.211(25)		
$^{Q}R(7,1)_a$	809.922816(14)	1.0729(88)	0.0583(29)	0.211(25)		
$^{Q}R(8,6)_a$	812.453286(20)	0.8137(64)	0.0841*	0.444*		
$^{Q}R(8,4)_a$	824.513073(32)	0.4640(60)	0.0715*	0.347*		
$^{Q}R(9,9)_a$	824.565969(31)	0.5227(63)	0.1044*	0.500*		
$^{Q}R(8,3)_a$	829.255019(16)	0.8901(87)	0.0678(43)	0.197(30)		
$^{Q}R(8,2)_a$	832.968616(30)	0.4860(59)	0.0598*	0.268*		
$^{Q}R(8,1)_a$	835.509364(26)	0.5650(59)	0.0542*	0.237*		
$^{Q}R(8,0)_a$	836.282482(13)	1.1547(88)	0.0587(27)	0.212(23)		

${}^{Q}R(10,10)_a$	840.948084(105)	0.1530(61)	0.0906*	0.500*		
${}^{Q}R(9,7)_a$	844.942328(52)	0.3120(62)	0.0906*	0.500*		
${}^{Q}R(9,6)_a$	852.462160(19)	0.5657(41)	0.0841*	0.500*		
${}^{Q}R(10,9)_a$	853.071027(29)	0.3634(40)	0.1044*	0.500*		
${}^{Q}R(9,2)_a$	858.383807(47)	0.1977(55)	0.0357(51)	0.241(87)		
${}^{Q}R(9,1)_a$	861.453874(45)	0.2342(39)	0.0542*	0.500*		
${}^{Q}R(9,3)_a$	865.466232(33)	0.3237(40)	0.0655*	0.500*		
${}^{Q}R(11,10)_a$	870.178045(123)	0.0864(39)	0.0906*	0.500*		
${}^{Q}R(12,12)_a$	872.993404(124)	0.0856(39)	0.0906*	0.500*		
${}^{Q}R(10,6)_a$	878.630779(37)	0.2878(40)	0.0841*	0.500*		
${}^{Q}R(11,9)_a$	881.329357(56)	0.1907(39)	0.1044*	0.500*		
${}^{Q}R(10,5)_a$	883.925405(95)	0.1129(39)	0.0777*	0.500*		
${}^{Q}R(10,4)_a$	887.647643(88)	0.1217(39)	0.0715*	0.500*		
${}^{Q}R(10,0)_a$	889.362017(54)	0.1989(39)	0.0488*	0.500*		
${}^{Q}R(10,3)_a$	889.737793(59)	0.1825(39)	0.0655*	0.500*		
${}^{Q}R(10,2)_a$	890.701002(137)	0.0782(39)	0.0598*	0.500*		
${}^{Q}R(10,1)_a$	890.715024(163)	0.0660(39)	0.0542*	0.500*		
${}^{Q}R(11,8)_a$	890.850835(120)	0.0901(39)	0.0974*	0.500*		
${}^{Q}R(11,7)_a$	898.818823(128)	0.0844(39)	0.0906*	0.500*		
${}^{Q}R(11,6)_a$	905.245327(80)	0.1255(36)	0.0841*	0.500*		
${}^{Q}R(12,9)_a$	909.650602(117)	0.0861(36)	0.1044*	0.500*		
${}^{Q}R(11,5)_a$	910.146311(192)	0.0538(36)	0.0777*	0.500*		
${}^{Q}R(11,3)_a$	915.931090(109)	0.0934(36)	0.0655*	0.500*		
${}^{Q}R(12,6)_a$	932.447315(230)	0.0363(32)	0.0841*	0.500*		
${}^{Q}R(12,5)_a$	937.146959(504)	0.0186(33)	0.0777*	0.500*		

Table S4. Measured parameters at 296 K for lines (labelled ${}^{\Delta K}\Delta J(J'',K'')_{i''}$) of the transition $2\nu_2(a) \leftarrow \nu_2(s)$. The numbers in parentheses are 1σ uncertainties in the units of the last digit listed. Missing entries indicate a lack of convergence for a given parameter, which was set to zero in the final solution. An asterisk (*) indicates that the line parameter was fixed to its value in HITRAN 2020.

Line	ν_0 cm-1	$S \times 10^{21}$ cm-1 / (mol. cm-2))	γ^0_{air} cm-1/atm	γ^0_{self} cm-1/atm	δ^0_{air} cm-1/atm	δ^0_{self} cm-1/atm
${}^{Q}P(11,6)_s$	710.088123(492)	0.0333(59)	0.0841*	0.500*		
${}^{Q}P(11,9)_s$	725.579871(241)	0.0633(59)	0.1044*	0.500*		
${}^{Q}P(10,2)_s$	725.719265(386)	0.0396(59)	0.0598*	0.500*		
${}^{Q}P(10,3)_s$	727.006822(129)	0.1165(59)	0.0655*	0.500*		
${}^{Q}P(10,4)_s$	728.895841(204)	0.0739(59)	0.0715*	0.500*		
${}^{Q}P(10,5)_s$	731.498824(209)	0.0732(59)	0.0777*	0.500*		
${}^{Q}P(10,6)_s$	734.952883(99)	0.1523(60)	0.0841*	0.500*		
${}^{Q}P(10,7)_s$	739.437476(173)	0.0877(59)	0.0906*	0.500*		
${}^{Q}P(10,8)_s$	745.185731(286)	0.0551(61)	0.0974*	0.500*		
${}^{Q}P(9,0)_s$	748.394717(54)	0.2858(60)	0.0488*	0.500*		
${}^{Q}P(9,1)_s$	748.684923(109)	0.1398(59)	0.0542*	0.500*		
${}^{Q}P(9,2)_s$	749.529832(111)	0.1376(59)	0.0598*	0.500*		
${}^{Q}P(9,3)_s$	750.987077(55)	0.2785(60)	0.0655*	0.500*		
${}^{Q}P(10,9)_s$	752.494378(198)	0.0769(59)	0.1044*	0.500*		
${}^{Q}P(9,4)_s$	753.135292(97)	0.1567(60)	0.0715*	0.500*		
${}^{Q}P(9,5)_s$	756.077607(118)	0.1290(60)	0.0777*	0.500*		
${}^{Q}P(9,6)_s$	759.962356(50)	0.3079(61)	0.0841*	0.500*		
${}^{Q}P(9,7)_s$	764.984155(112)	0.1369(60)	0.0906*	0.500*		
${}^{Q}P(9,8)_s$	771.391220(159)	0.0973(60)	0.0974*	0.500*		
${}^{Q}P(8,1)_s$	772.439961(49)	0.2817(57)	0.0629*	0.253*		
${}^{Q}P(8,2)_s$	773.385736(48)	0.2943(58)	0.0683*	0.296*		
${}^{Q}P(8,3)_s$	775.015547(24)	0.5709(86)	0.0683(68)	0.224(45)		
${}^{Q}P(8,4)_s$	777.403790(50)	0.2959(59)	0.0798*	0.397*		
${}^{Q}P(8,5)_s$	780.669209(54)	0.2831(60)	0.0858*	0.455*		
${}^{Q}P(8,6)_s$	784.967419(29)	0.4446(85)	0.0688(112)	0.086(54)		
${}^{Q}P(8,7)_s$	790.502822(102)	0.1600(61)	0.0985*	0.585*		
${}^{Q}P(7,0)_s$	795.770280(13)	1.0790(87)	0.0718(38)	0.224(25)		
${}^{Q}P(7,1)_s$	796.117352(27)	0.5276(61)	0.0710*	0.274*		
${}^{Q}P(7,2)_s$	797.157505(27)	0.5476(88)	0.0647(66)	0.339(50)		
${}^{Q}P(7,3)_s$	798.944767(14)	1.0462(89)	0.0726(40)	0.289(26)		
${}^{Q}P(7,4)_s$	801.563362(30)	0.4689(87)	0.0780(100)	0.240(55)		
${}^{Q}P(7,5)_s$	805.132853(35)	0.4268(89)	0.0821(117)	0.372(65)		

${}^{Q}P(7,6)_s$	809.818281(27)	0.5562(90)	0.3341(778)	0.346(50)		
${}^{Q}P(6,1)_s$	819.591173(16)	0.8641(85)	0.0616(38)	0.126(29)		
${}^{Q}P(6,2)_s$	820.717793(17)	0.8571(87)	0.0635(41)	0.180(30)		
${}^{Q}P(6,3)_s$	822.651909(10)	1.6059(90)	0.0722(26)	0.266(18)		
${}^{Q}P(6,4)_s$	825.479494(22)	0.6969(89)	0.0839(74)	0.323(40)		
${}^{Q}P(6,5)_s$	829.327782(34)	0.4791(92)	0.0853(112)	0.514(63)		
${}^{Q}P(5,0)_s$	842.343225(6)	2.7273(93)	0.0764(17)	0.226(11)		
${}^{Q}P(5,1)_s$	842.740810(11)	1.3393(89)	0.0714(31)	0.236(21)		
${}^{Q}P(5,2)_s$	843.944460(12)	1.2223(89)	0.0806(40)	0.218(22)		
${}^{Q}P(5,3)_s$	846.008747(8)	2.0508(91)	0.0872(27)	0.212(14)		
${}^{Q}P(5,4)_s$	849.023880(22)	0.6653(89)	0.0999(100)	0.262(41)		
${}^{Q}P(4,1)_s$	865.454592(6)	1.7072(57)	0.0827(19)	0.160(11)		
${}^{Q}P(4,2)_s$	866.724716(7)	1.4571(57)	0.0892(25)	0.201(12)		
${}^{Q}P(4,3)_s$	868.901652(5)	1.8645(58)	0.0893(19)	0.205(10)		
${}^{Q}P(3,0)_s$	887.200086(3)	3.9724(63)	0.0832(8)	0.212(5)		
${}^{Q}P(3,1)_s$	887.633270(6)	1.8362(58)	0.0847(20)	0.190(10)		
${}^{Q}P(3,2)_s$	888.958065(8)	1.2126(57)	0.0968(33)	0.193(15)		
${}^{Q}P(2,1)_s$	909.192813(7)	1.4081(54)	0.0884(26)	0.294(13)		
${}^{Q}Q(11,6)_s$	921.827274(174)	0.0587(37)	0.0841*	0.500*		
${}^{Q}Q(10,5)_s$	924.205943(190)	0.0549(36)	0.0777*	0.500*		
${}^{Q}Q(9,3)_s$	924.566046(130)	0.0785(36)	0.0655*	0.500*		
${}^{Q}Q(9,4)_s$	926.753115(121)	0.0838(36)	0.0715*	0.500*		
${}^{Q}Q(10,6)_s$	927.719583(53)	0.1920(37)	0.0841*	0.500*		
${}^{Q}Q(8,3)_s$	929.491139(47)	0.2035(36)	0.0740*	0.344*		
${}^{Q}P(1,0)_s$	929.607880(4)	2.3206(56)	0.0926(21)	0.285(8)		
${}^{Q}Q(9,5)_s$	929.736289(70)	0.1468(37)	0.0777*	0.500*		
${}^{Q}Q(12,9)_s$	929.886426(119)	0.1045(48)	0.1044*	0.500*		
${}^{Q}Q(11,8)_s$	930.995865(121)	0.0850(37)	0.0974*	0.500*		
${}^{Q}Q(8,4)_s$	931.904955(46)	0.2113(36)	0.0798*	0.397*		
${}^{Q}Q(10,7)_s$	932.264439(67)	0.1514(37)	0.0906*	0.500*		
${}^{Q}Q(7,2)_s$	932.439494(95)	0.0989(35)	0.0763*	0.328*		
${}^{Q}Q(9,6)_s$	933.665012(2)	0.5211(38)	0.0841*	0.500*		
${}^{Q}Q(7,3)_s$	934.241006(3)	0.5656(114)	0.0435(46)	0.303(50)		
${}^{Q}Q(8,5)_s$	935.200579(3)	0.3906(37)	0.0858*	0.455*		
${}^{Q}Q(6,1)_s$	935.635463(20)	0.0719(43)	0.0786*	0.299*		
${}^{Q}Q(6,2)_s$	936.769123(4)	0.2329(36)	0.0837*	0.364*		
${}^{Q}Q(7,4)_s$	936.879574(2)	0.5001(53)	0.0770(60)	0.236(34)		
${}^{Q}Q(12,10)_s$	937.111965(13)	0.0652(33)	0.0906*	0.031*		
${}^{Q}Q(11,9)_s$	937.553324(4)	0.2844(37)	0.1044*	0.500*		
${}^{Q}Q(10,8)_s$	938.068137(4)	0.2592(37)	0.0974*	0.500*		
${}^{Q}Q(6,3)_s$	938.714431(1)	1.1247(54)	0.0815(34)	0.242(16)		
${}^{Q}Q(9,7)_s$	938.728735(2)	0.4176(53)	0.0551(52)	0.239(41)		
${}^{Q}Q(5,1)_s$	939.509750(9)	0.1068(35)	0.0855*	0.327*		
${}^{Q}Q(8,6)_s$	939.529244(1)	1.2942(54)	0.0723(24)	0.199(13)		
${}^{Q}Q(7,5)_s$	940.470182(1)	0.9026(54)	0.0785(34)	0.246(19)		
${}^{Q}Q(5,2)_s$	940.718497(2)	0.4981(37)	0.0905*	0.404*		
${}^{Q}Q(6,4)_s$	941.555109(1)	1.1055(53)	0.0765(27)	0.205(16)		
${}^{Q}Q(5,3)_s$	942.790100(1)	2.3358(55)	0.0874(15)	0.222(8)	0.00851(151)	0.091(16)
${}^{Q}Q(4,1)_s$	942.911049(14)	0.1947(432)	0.0919*	0.360*		
${}^{Q}Q(4,2)_s$	944.184530(1)	0.9435(53)	0.0765(31)	0.200(18)		
${}^{Q}Q(8,7)_s$	945.091674(1)	1.1082(53)	0.0807(31)	0.191(16)		
${}^{Q}Q(9,8)_s$	945.169853(2)	0.6950(77)	0.0784(74)	0.209(32)		
${}^{Q}Q(7,6)_s$	945.175672(1)	3.1878(79)	0.0812(15)	0.241(8)	0.00689(128)	0.071(13)
${}^{Q}Q(6,5)_s$	945.417486(2)	2.0230(56)	0.0736(14)	0.149(9)	0.01051(137)	0.162(19)
${}^{Q}Q(3,1)_s$	945.748928(2)	0.4381(53)	0.0962(102)	0.233(39)		
${}^{Q}Q(5,4)_s$	945.814174(1)	2.3799(56)	0.0842(14)	0.255(8)	0.01161(153)	0.085(16)
${}^{Q}Q(11,10)_s$	945.864833(4)	0.2516(37)	0.0906*	0.500*		
${}^{Q}Q(4,3)_s$	946.366253(1)	4.6392(60)	0.0873(8)	0.224(4)	0.00719(76)	0.116(9)
${}^{Q}Q(12,11)_s$	946.455597(9)	0.1178(37)	0.0906*	0.500*		
${}^{Q}Q(3,2)_s$	947.075802(1)	1.7990(55)	0.0951(22)	0.212(10)		
${}^{Q}Q(13,12)_s$	947.303743(8)	0.1247(37)	0.0906*	0.500*		
${}^{Q}Q(2,1)_s$	947.947355(1)	0.8179(54)	0.0866(44)	0.312(22)		
${}^{Q}Q(2,2)_s$	949.315285(1)	3.4462(58)	0.0889(13)	0.258(6)	0.01084(129)	0.114(12)
${}^{Q}Q(3,3)_s$	949.348205(0)	8.8365(75)	0.0911(5)	0.249(3)	0.00808(54)	0.113(6)
${}^{Q}Q(1,1)_s$	949.447151(1)	1.7729(55)	0.0907(24)	0.238(10)		
${}^{Q}Q(4,4)_s$	949.548159(1)	4.6811(61)	0.0888(8)	0.241(4)	0.01010(81)	0.097(9)
${}^{Q}Q(5,5)_s$	949.919693(1)	4.3280(59)	0.0870(8)	0.220(5)	0.00560(82)	0.099(10)
${}^{Q}Q(6,6)_s$	950.469740(1)	7.1868(68)	0.0862(5)	0.238(3)	0.00668(49)	0.113(7)
${}^{Q}Q(7,7)_s$	951.207494(1)	2.7302(56)	0.0822(12)	0.221(7)	0.01079(119)	0.115(14)
${}^{Q}Q(8,8)_s$	952.144550(1)	1.8995(55)	0.0833(18)	0.222(10)		
${}^{Q}Q(9,9)_s$	953.294476(1)	2.4602(56)	0.0835(14)	0.210(8)	0.00611(135)	0.097(16)

$^{Q}Q(10,10)_s$	954.674406(1)	0.7222(53)	0.0835(46)	0.140(23)		
$^{Q}Q(11,11)_s$	956.298570(2)	0.4479(54)	0.1140(127)	0.324(40)		
$^{Q}Q(12,12)_s$	958.196579(2)	0.4434(54)	0.0692(61)	0.323(40)		
$^{Q}Q(13,13)_s$	960.402071(9)	0.1140(37)	0.9060*	0.500*		
$^{Q}R(1,0)_s$	987.742173(1)	4.8242(62)	0.0926(8)	0.282(4)	0.00711(80)	0.121(9)
$^{Q}R(1,1)_s$	988.201702(1)	1.8170(56)	0.0924(21)	0.248(10)		
$^{Q}R(2,1)_s$	1006.063053(0)	2.7196(61)	0.0880(14)	0.263(8)		
$^{Q}R(2,2)_s$	1007.433122(1)	1.8047(60)	0.1048(34)	0.229(11)		
$^{Q}R(3,0)_s$	1022.770370(0)	5.9880(68)	0.0821(6)	0.191(4)		
$^{Q}R(3,1)_s$	1023.205436(0)	2.9505(61)	0.0881(12)	0.202(7)		
$^{Q}R(3,2)_s$	1024.535633(0)	2.4920(60)	0.0898(15)	0.216(9)		
$^{Q}R(3,3)_s$	1026.813005(0)	3.1792(62)	0.0906(13)	0.235(7)		
$^{Q}R(4,1)_s$	1039.680185(0)	2.5996(60)	0.0768(12)	0.181(8)		
$^{Q}R(4,2)_s$	1040.958522(0)	2.4129(60)	0.0825(14)	0.207(9)		
$^{Q}R(4,3)_s$	1043.147717(0)	4.0239(63)	0.0888(9)	0.215(6)		
$^{Q}R(4,4)_s$	1046.338521(1)	1.2789(61)	0.1322(90)	0.234(17)		
$^{Q}R(5,0)_s$	1055.152487(0)	4.0136(64)	0.0734(7)	0.213(6)		
$^{Q}R(5,1)_s$	1055.554218(1)	2.0082(60)	0.0749(15)	0.255(11)		
$^{Q}R(5,2)_s$	1056.769864(1)	1.9255(60)	0.0829(18)	0.204(11)		
$^{Q}R(5,3)_s$	1058.852664(0)	3.5305(62)	0.0844(10)	0.202(6)		
$^{Q}R(5,4)_s$	1061.889838(1)	1.4867(59)	0.0805(22)	0.211(14)		
$^{Q}R(5,5)_s$	1066.009336(1)	1.0334(44)	0.1003*	0.591*		
$^{Q}R(6,1)_s$	1070.907505(1)	1.3291(58)	0.0686(20)	0.155(15)		
$^{Q}R(6,2)_s$	1072.050891(1)	1.3176(59)	0.0714(21)	0.217(16)		
$^{Q}R(6,3)_s$	1074.010737(0)	2.5838(61)	0.0870(15)	0.208(8)		
$^{Q}R(6,4)_s$	1076.871336(1)	1.2237(59)	0.0757(24)	0.228(17)		
$^{Q}R(6,5)_s$	1080.754666(1)	1.0302(58)	0.0817(32)	0.179(20)		
$^{Q}R(7,0)_s$	1085.475021(1)	1.6233(60)	0.0720(17)	0.239(13)		
$^{Q}R(6,6)_s$	1085.827182(3)	1.3576(270)	0.0961(32)	0.239(25)		
$^{Q}R(7,1)_s$	1085.829991(4)	0.8098(244)	0.0629*	0.253*		
$^{Q}R(7,2)_s$	1086.892907(1)	0.8235(41)	0.0683*	0.296*		
$^{Q}R(7,3)_s$	1088.716839(1)	1.6134(60)	0.0805(20)	0.213(13)		
$^{Q}R(7,4)_s$	1091.380552(1)	0.8160(42)	0.0798*	0.397*		
$^{Q}R(7,5)_s$	1095.001392(2)	0.8027(42)	0.0858*	0.455*		
$^{Q}R(7,6)_s$	1099.737581(1)	1.3409(60)	0.0793(24)	0.266(16)		
$^{Q}R(8,1)_s$	1100.417934(3)	0.4251(39)	0.0542*	0.237*		
$^{Q}R(8,2)_s$	1101.393898(3)	0.4369(39)	0.0598*	0.268*		
$^{Q}R(8,3)_s$	1103.070194(1)	0.9365(41)	0.0655*	0.305*		
$^{Q}R(8,4)_s$	1105.522193(2)	0.4691(40)	0.0715*	0.347*		
$^{Q}R(7,7)_s$	1105.796327(3)	0.4825(42)	0.0984*	0.585*		
$^{Q}R(8,5)_s$	1108.859423(2)	0.4745(40)	0.0777*	0.393*		
$^{Q}R(8,6)_s$	1113.232036(1)	0.9348(42)	0.0841*	0.444*		
$^{Q}R(9,0)_s$	1114.468002(3)	0.4410(41)	0.0488*	0.500*		
$^{Q}R(9,1)_s$	1114.771285(5)	0.2243(40)	0.0542*	0.500*		
$^{Q}R(9,2)_s$	1115.654936(5)	0.2391(40)	0.0598*	0.500*		
$^{Q}R(9,3)_s$	1117.176450(3)	0.4649(41)	0.0655*	0.500*		
$^{Q}R(8,7)_s$	1118.836201(3)	0.4107(41)	0.0906*	0.500*		
$^{Q}R(9,4)_s$	1119.404871(5)	0.2381(41)	0.0715*	0.500*		
$^{Q}R(9,5)_s$	1122.443017(5)	0.2510(41)	0.0777*	0.500*		
$^{Q}R(8,8)_s$	1118.836201(3)	0.3069(41)	0.0974*	0.561*		
$^{Q}R(9,6)_s$	1126.431792(2)	0.5180(42)	0.0841*	0.500*		
$^{Q}R(10,1)_s$	1128.989137(13)	0.0938(40)	0.0542*	0.500*		
$^{Q}R(10,2)_s$	1129.776736(13)	0.0956(40)	0.0598*	0.500*		
$^{Q}R(10,3)_s$	1131.139102(6)	0.2103(40)	0.0655*	0.500*		
$^{Q}R(9,7)_s$	1131.555782(5)	0.2651(41)	0.0906*	0.500*		
$^{Q}R(10,4)_s$	1133.136619(14)	0.0896(40)	0.0715*	0.500*		
$^{Q}R(10,5)_s$	1135.866206(12)	0.1016(40)	0.0777*	0.500*		
$^{Q}R(9,8)_s$	1138.051771(5)	0.2438(41)	0.0974*	0.500*		
$^{Q}R(10,6)_s$	1139.458876(6)	0.2393(45)	0.0841*	0.500*		
$^{Q}R(11,0)_s$	1142.914228(19)	0.0645(40)	0.0488*	0.500*		
$^{Q}R(10,7)_s$	1144.086796(10)	0.1238(40)	0.0906*	0.500*		
$^{Q}R(11,3)_s$	1145.054603(15)	0.0810(40)	0.0655*	0.500*		
$^{Q}R(9,9)_s$	1146.218079(4)	0.3502(41)	0.1044*	0.500*		
$^{Q}R(10,8)_s$	1149.970958(10)	0.1198(41)	0.0974*	0.500*		
$^{Q}R(11,6)_s$	1152.433842(10)	0.1258(41)	0.0841*	0.500*		
$^{Q}R(11,7)_s$	1156.564717(59)	0.0682(267)	0.0906*	0.500*		
$^{Q}R(10,9)_s$	1157.391155(4)	0.2824(41)	0.1044*	0.500*		
$^{Q}R(11,8)_s$	1161.827639(20)	0.0626(40)	0.0974*	0.500*		
$^{Q}R(10,10)_s$	1166.710893(17)	0.0765(41)	0.0906*	0.500*		
$^{Q}R(11,9)_s$	1168.504894(10)	0.1335(41)	0.1044*	0.500*		
$^{Q}R(11,10)_s$	1176.783247(18)	0.0716(41)	0.0906*	0.500*		

Table S5. Measured parameters at 296 K for lines (labelled ${}^{\Delta K}\Delta J(J'',K'')_{i''}$) of the $^{15}NH_3$ isotopologue transition $\nu_2(s) \leftarrow GS(a)$. The numbers in parentheses are 1σ uncertainties in the units of the last digit listed.

Line	$\boldsymbol{\nu_0}$ cm^{-1}	$\boldsymbol{S} \times 10^{21}$ cm^{-1} / (mol. cm^{-2}))
${}^{Q}P(10,6)_a$	733.24967(25)	0.0609(59)
${}^{Q}P(9,7)_a$	746.49702(31)	0.0515(62)
${}^{Q}P(9,6)_a$	750.23976(26)	0.0577(59)
${}^{Q}P(9,5)_a$	753.24274(35)	0.0434(59)
${}^{Q}P(9,3)_a$	757.36556(24)	0.0640(59)
${}^{Q}P(9,1)_a$	759.31857(45)	0.0333(59)
${}^{Q}P(8,7)_a$	763.57666(34)	0.0476(60)
${}^{Q}P(8,6)_a$	767.47091(16)	0.0932(60)
${}^{Q}P(8,5)_a$	770.59547(23)	0.0650(59)
${}^{Q}P(8,4)_a$	773.04122(22)	0.0666(58)
${}^{Q}P(8,2)_a$	776.15480(19)	0.0732(56)
${}^{Q}P(8,1)_a$	776.90628(28)	0.0501(56)
${}^{Q}P(8,0)_a$	777.16020(11)	0.1255(55)
${}^{Q}P(7,5)_a$	788.21031(19)	0.0818(60)
${}^{Q}P(7,4)_a$	790.73882(13)	0.1156(59)
${}^{Q}P(7,3)_a$	792.63644(6)	0.2307(59)
${}^{Q}P(7,2)_a$	793.95527(12)	0.1167(57)
${}^{Q}P(7,1)_a$	794.73187(13)	0.1068(57)
${}^{Q}P(6,5)_a$	806.11542(15)	0.1056(61)
${}^{Q}P(6,4)_a$	808.71429(10)	0.1513(60)
${}^{Q}P(6,3)_a$	810.66343(4)	0.3673(61)
${}^{Q}P(6,2)_a$	812.01878(7)	0.2034(59)
${}^{Q}P(6,1)_a$	812.81716(6)	0.2225(58)
${}^{Q}P(6,0)_a$	813.08251(3)	0.4157(58)
${}^{Q}P(5,4)_a$	826.98903(9)	0.1745(62)
${}^{Q}P(5,3)_a$	828.98052(3)	0.4917(62)
${}^{Q}P(5,2)_a$	830.36420(5)	0.2944(60)
${}^{Q}P(5,1)_a$	831.17963(5)	0.3138(59)
${}^{Q}P(4,3)_a$	847.60101(4)	0.4284(64)
${}^{Q}P(4,2)_a$	849.00583(4)	0.3554(61)
${}^{Q}P(4,1)_a$	849.83331(4)	0.4134(60)
${}^{Q}P(4,0)_a$	850.10683(1)	0.8439(40)
${}^{Q}P(3,2)_a$	867.95194(4)	0.3010(41)
${}^{Q}P(3,1)_a$	868.78657(2)	0.4243(39)
${}^{Q}P(2,1)_a$	888.04122(3)	0.3458(40)
${}^{Q}P(2,0)_a$	888.31743(1)	0.8937(41)
${}^{Q}Q(12,12)_a$	908.70577(10)	0.0998(36)
${}^{Q}Q(11,11)_a$	911.94686(9)	0.1074(36)
${}^{Q}Q(13,12)_a$	912.82073(36)	0.0285(36)
${}^{Q}Q(10,10)_a$	914.86360(6)	0.1689(36)
${}^{Q}Q(12,11)_a$	915.61297(39)	0.0269(36)
${}^{Q}Q(9,9)_a$	917.46522(2)	0.5589(38)
${}^{Q}Q(11,10)_a$	918.11634(18)	0.0583(36)
${}^{Q}Q(8,8)_a$	919.75946(2)	0.4610(39)
${}^{Q}Q(10,9)_a$	920.33616(5)	0.2023(37)
${}^{Q}Q(12,10)_a$	921.31406(40)	0.0255(36)
${}^{Q}Q(7,7)_a$	921.75369(2)	0.6679(40)
${}^{Q}Q(9,8)_a$	922.27635(6)	0.1636(36)
${}^{Q}Q(11,9)_a$	923.20491(18)	0.0562(36)
${}^{Q}Q(6,6)_a$	923.45400(1)	1.7431(43)
${}^{Q}Q(8,7)_a$	923.94072(4)	0.2733(38)
${}^{Q}Q(10,8)_a$	924.83855(15)	0.0664(36)
${}^{Q}Q(5,5)_a$	924.86556(1)	1.0604(41)
${}^{Q}Q(7,6)_a$	925.33189(1)	0.7691(39)
${}^{Q}Q(4,4)_a$	925.99246(1)	1.1238(41)
${}^{Q}Q(9,7)_a$	926.21528(10)	0.1053(36)
${}^{Q}Q(6,5)_a$	926.45141(2)	0.4957(38)
${}^{Q}Q(3,3)_a$	926.83776(1)	2.1307(44)
${}^{Q}Q(5,4)_a$	927.29996(2)	0.5834(42)
${}^{Q}Q(8,6)_a$	927.33374(5)	0.3147(63)
${}^{Q}Q(2,2)_a$	927.40342(1)	0.8385(40)
${}^{Q}Q(1,1)_a$	927.69050(2)	0.4325(38)
${}^{Q}Q(4,3)_a$	927.87704(1)	1.1230(40)

${}^{Q}Q(3,2)_a$	928.18146(2)	0.4368(38)
${}^{Q}Q(7,5)_a$	928.19287(5)	0.2195(37)
${}^{Q}Q(2,1)_a$	928.21050(5)	0.2151(37)
${}^{Q}Q(10,7)_a$	928.52519(27)	0.0386(36)
${}^{Q}Q(6,4)_a$	928.79027(4)	0.2898(38)
${}^{Q}Q(3,1)_a$	928.97270(10)	0.0966(36)
${}^{Q}Q(5,3)_a$	929.12290(2)	0.5377(38)
${}^{Q}Q(4,2)_a$	929.18545(5)	0.2090(38)
${}^{Q}Q(9,6)_a$	929.41176(9)	0.1174(36)
${}^{Q}Q(4,1)_a$	929.95570(21)	0.0481(36)
${}^{Q}Q(8,5)_a$	930.04684(11)	0.0887(36)
${}^{Q}Q(5,2)_a$	930.38798(9)	0.1117(36)
${}^{Q}Q(7,4)_a$	930.42549(8)	0.1236(36)
${}^{Q}Q(6,3)_a$	930.54106(4)	0.2638(36)
${}^{Q}Q(5,1)_a$	931.13259(53)	0.0208(38)
${}^{Q}Q(10,6)_a$	931.51859(20)	0.0526(36)
${}^{Q}Q(6,2)_a$	931.75710(15)	0.0679(39)
${}^{Q}Q(9,5)_a$	931.96864(25)	0.0412(36)
${}^{Q}Q(7,3)_a$	932.09860(14)	0.1509(134)
${}^{Q}Q(8,4)_a$	932.16458(23)	0.0439(36)
${}^{Q}Q(8,3)_a$	933.74629(26)	0.0372(35)
${}^{Q}R(0,0)_a$	947.79211(2)	0.6453(38)
${}^{Q}R(1,1)_a$	967.85962(2)	0.4338(38)
${}^{Q}R(2,2)_a$	987.63286(3)	0.4153(38)
${}^{Q}R(2,1)_a$	988.39626(2)	0.6751(38)
${}^{Q}R(2,0)_a$	988.64850(1)	1.4582(40)
${}^{Q}R(3,3)_a$	1007.11373(2)	0.7800(42)
${}^{Q}R(3,2)_a$	1008.36093(2)	0.6013(41)
${}^{Q}R(3,1)_a$	1009.09456(2)	0.7064(41)
${}^{Q}R(4,4)_a$	1026.30317(4)	0.3126(41)
${}^{Q}R(4,3)_a$	1028.01951(1)	0.9783(43)
${}^{Q}R(4,2)_a$	1029.20912(2)	0.5708(41)
${}^{Q}R(4,1)_a$	1029.90877(2)	0.6132(40)
${}^{Q}R(4,0)_a$	1030.14119(1)	1.2541(42)
${}^{Q}R(5,5)_a$	1045.20128(6)	0.2250(41)
${}^{Q}R(5,4)_a$	1047.37591(3)	0.3650(41)
${}^{Q}R(5,3)_a$	1049.00054(1)	0.8352(42)
${}^{Q}R(5,2)_a$	1050.12681(2)	0.4663(40)
${}^{Q}R(5,1)_a$	1050.78887(2)	0.4706(39)
${}^{Q}R(6,6)_a$	1063.80670(4)	0.3314(42)
${}^{Q}R(6,5)_a$	1066.43351(5)	0.2521(41)
${}^{Q}R(6,4)_a$	1068.47692(4)	0.2859(40)
${}^{Q}R(6,3)_a$	1070.00350(2)	0.5935(41)
${}^{Q}R(6,2)_a$	1071.06053(4)	0.2964(39)
${}^{Q}R(6,1)_a$	1071.68182(3)	0.3160(39)
${}^{Q}R(6,0)_a$	1071.89176(2)	0.6108(39)
${}^{Q}R(7,7)_a$	1082.11731(10)	0.1279(41)
${}^{Q}R(7,6)_a$	1085.19406(4)	0.3200(41)
${}^{Q}R(7,5)_a$	1087.64367(7)	0.1805(40)
${}^{Q}R(7,4)_a$	1089.54839(6)	0.1881(40)
${}^{Q}R(7,3)_a$	1090.96948(3)	0.3721(40)
${}^{Q}R(7,2)_a$	1091.95511(6)	0.1807(39)
${}^{Q}R(7,1)_a$	1092.53329(6)	0.1758(38)
${}^{Q}R(8,8)_a$	1100.12918(17)	0.0740(41)
${}^{Q}R(8,7)_a$	1103.65823(14)	0.0888(41)
${}^{Q}R(8,6)_a$	1106.50583(6)	0.2154(40)
${}^{Q}R(8,5)_a$	1108.77102(13)	0.0943(39)
${}^{Q}R(8,4)_a$	1110.53173(11)	0.1087(39)
${}^{Q}R(8,3)_a$	1111.84695(6)	0.2026(39)
${}^{Q}R(8,2)_a$	1112.75514(12)	0.0960(38)
${}^{Q}R(8,1)_a$	1113.28825(10)	0.1076(38)
${}^{Q}R(8,0)_a$	1113.47597(5)	0.1948(38)
${}^{Q}R(9,9)_a$	1117.84043(12)	0.0982(40)
${}^{Q}R(9,8)_a$	1121.82750(16)	0.0781(40)
${}^{Q}R(9,7)_a$	1125.06645(18)	0.0658(40)
${}^{Q}R(9,6)_a$	1127.67940(11)	0.1078(40)
${}^{Q}R(9,5)_a$	1129.75711(24)	0.0511(40)
${}^{Q}R(9,4)_a$	1131.37020(28)	0.0439(40)
${}^{Q}R(9,3)_a$	1132.57209(10)	0.1169(40)
${}^{Q}R(9,2)_a$	1133.40787(19)	0.0629(40)
${}^{Q}R(9,1)_a$	1133.89331(23)	0.0525(40)

${}^{Q}R(10,10)_a$	1135.24398(34)	0.0386(41)
${}^{Q}R(10,9)_a$	1139.69694(17)	0.0737(40)
${}^{Q}R(10,8)_a$	1143.32973(52)	0.0251(40)
${}^{Q}R(10,7)_a$	1146.27840(75)	0.0173(40)
${}^{Q}R(10,6)_a$	1148.65528(23)	0.0534(40)
${}^{Q}R(10,5)_a$	1150.54420(50)	0.0256(40)
${}^{Q}R(10,4)_a$	1152.00917(123)	0.0128(40)
${}^{Q}R(10,3)_a$	1153.10666(40)	0.0317(40)
${}^{Q}R(10,0)_a$	1154.46826(23)	0.0534(40)
${}^{Q}R(11,9)_a$	1161.29341(65)	0.0207(41)
${}^{Q}R(11,6)_a$	1169.37718(63)	0.0207(41)

Table S6. Measured parameters at 296 K for lines (labelled ${}^{\Delta K}\Delta J(J'', K'')_{i''}$) of the $^{15}NH_3$ isotopologue transition $\nu_2(a) \leftarrow GS(s)$. The numbers in parentheses are 1σ uncertainties in the units of the last digit listed.

Line	$\boldsymbol{\nu_0}$ cm^{-1}	$\boldsymbol{S} \times 10^{21}$ cm^{-1} / (mol. cm^{-2}))
${}^{Q}P(10,6)_s$	761.78486(64)	0.0245(59)
${}^{Q}P(10,3)_s$	763.48584(26)	0.0601(59)
${}^{Q}P(9,7)_s$	780.91193(48)	0.0328(60)
${}^{Q}P(9,6)_s$	781.58062(34)	0.0458(59)
${}^{Q}P(9,5)_s$	782.18428(40)	0.0395(59)
${}^{Q}P(9,3)_s$	783.11458(20)	0.0768(59)
${}^{Q}P(9,2)_s$	783.41870(42)	0.0362(59)
${}^{Q}P(9,1)_s$	783.60028(43)	0.0366(59)
${}^{Q}P(9,0)_s$	783.66355(22)	0.0707(59)
${}^{Q}P(8,7)_s$	800.95561(36)	0.0455(61)
${}^{Q}P(8,6)_s$	801.52872(12)	0.1289(60)
${}^{Q}P(8,5)_s$	802.05594(25)	0.0614(59)
${}^{Q}P(8,4)_s$	802.51393(22)	0.0669(58)
${}^{Q}P(8,3)_s$	802.88077(13)	0.1092(58)
${}^{Q}P(8,2)_s$	803.15805(16)	0.0890(57)
${}^{Q}P(8,1)_s$	803.32325(22)	0.0625(56)
${}^{Q}P(7,6)_s$	821.59886(12)	0.1334(62)
${}^{Q}P(7,5)_s$	822.04954(16)	0.1005(60)
${}^{Q}P(7,4)_s$	822.44802(15)	0.0995(59)
${}^{Q}P(7,3)_s$	822.77416(7)	0.2272(59)
${}^{Q}P(7,2)_s$	823.01660(14)	0.1064(58)
${}^{Q}P(7,1)_s$	823.16446(12)	0.1146(57)
${}^{Q}P(7,0)_s$	823.21434(6)	0.2282(57)
${}^{Q}P(6,5)_s$	842.13122(16)	0.1008(62)
${}^{Q}P(6,4)_s$	842.47101(10)	0.1610(61)
${}^{Q}P(6,3)_s$	842.75283(4)	0.3572(61)
${}^{Q}P(6,2)_s$	842.96566(7)	0.2090(59)
${}^{Q}P(6,1)_s$	843.09600(7)	0.2143(58)
${}^{Q}P(5,4)_s$	862.55008(7)	0.1501(39)
${}^{Q}P(5,3)_s$	862.79099(2)	0.4875(40)
${}^{Q}P(5,2)_s$	862.97342(4)	0.2758(38)
${}^{Q}P(5,1)_s$	863.08671(3)	0.3108(38)
${}^{Q}P(5,0)_s$	863.12514(2)	0.6026(39)
${}^{Q}P(4,3)_s$	882.85343(3)	0.4239(40)
${}^{Q}P(4,2)_s$	883.00848(3)	0.3329(39)
${}^{Q}P(4,1)_s$	883.10549(3)	0.3851(39)
${}^{Q}P(3,2)_s$	903.03953(3)	0.2910(55)
${}^{Q}P(3,1)_s$	903.12180(2)	0.4276(54)
${}^{Q}P(3,0)_s$	903.14989(1)	0.9471(54)
${}^{Q}P(2,1)_s$	923.10652(3)	0.3337(37)
${}^{Q}P(1,0)_s$	943.05321(2)	0.5937(37)
${}^{Q}Q(12,12)_s$	952.60993(10)	0.1043(36)
${}^{Q}Q(11,11)_s$	954.18428(11)	0.0922(36)
${}^{Q}Q(11,10)_s$	954.55528(18)	0.0569(36)
${}^{Q}Q(11,9)_s$	955.03170(14)	0.0705(36)
${}^{Q}Q(10,10)_s$	955.63373(6)	0.1726(37)
${}^{Q}Q(10,9)_s$	955.98087(5)	0.2031(37)
${}^{Q}Q(10,8)_s$	956.40210(14)	0.0930(55)
${}^{Q}Q(9,9)_s$	956.95651(2)	0.5567(38)
${}^{Q}Q(9,8)_s$	957.27408(6)	0.1683(37)

$^{Q}Q(9,7)_s$	957.64100(10)	0.0992(37)
$^{Q}Q(9,6)_s$	958.01619(8)	0.1210(37)
$^{Q}Q(8,8)_s$	958.15005(3)	0.4389(39)
$^{Q}Q(8,7)_s$	958.43437(4)	0.2748(38)
$^{Q}Q(8,6)_s$	958.74601(3)	0.2948(37)
$^{Q}Q(8,5)_s$	959.05185(11)	0.0955(36)
$^{Q}Q(7,7)_s$	959.21289(2)	0.5976(41)
$^{Q}Q(8,4)_s$	959.32757(21)	0.0464(35)
$^{Q}Q(7,6)_s$	959.46083(1)	0.7297(39)
$^{Q}Q(8,3)_s$	959.56240(19)	0.0521(35)
$^{Q}Q(7,5)_s$	959.71797(5)	0.2190(37)
$^{Q}Q(7,4)_s$	959.95729(9)	0.1148(36)
$^{Q}Q(6,6)_s$	960.14307(1)	1.6872(43)
$^{Q}Q(7,3)_s$	960.15420(9)	0.1131(36)
$^{Q}Q(6,5)_s$	960.35299(2)	0.4650(38)
$^{Q}Q(6,4)_s$	960.55690(4)	0.2756(37)
$^{Q}Q(6,3)_s$	960.73528(4)	0.2555(37)
$^{Q}Q(6,2)_s$	960.87008(17)	0.0587(36)
$^{Q}Q(5,5)_s$	960.93973(1)	1.0115(41)
$^{Q}Q(6,1)_s$	960.95646(95)	0.0139(42)
$^{Q}Q(5,4)_s$	961.11041(2)	0.5309(39)
$^{Q}Q(5,3)_s$	961.26176(2)	0.5388(38)
$^{Q}Q(5,2)_s$	961.38287(9)	0.1101(36)
$^{Q}Q(5,1)_s$	961.45809(23)	0.0415(35)
$^{Q}Q(4,4)_s$	961.60184(1)	1.0827(41)
$^{Q}Q(4,3)_s$	961.73309(1)	1.0820(40)
$^{Q}Q(4,2)_s$	961.83773(4)	0.2273(37)
$^{Q}Q(4,1)_s$	961.90447(16)	0.0614(35)
$^{Q}Q(3,3)_s$	962.12848(1)	2.0747(45)
$^{Q}Q(3,2)_s$	962.22069(2)	0.4147(38)
$^{Q}Q(2,2)_s$	962.51987(1)	0.7857(39)
$^{Q}Q(2,1)_s$	962.57380(5)	0.1940(36)
$^{Q}Q(1,1)_s$	962.77506(3)	0.4200(58)
$^{Q}R(1,1)_s$	1002.24232(3)	0.4152(40)
$^{Q}R(1,0)_s$	1002.25468(1)	1.1311(42)
$^{Q}R(2,2)_s$	1021.70107(3)	0.4312(41)
$^{Q}R(2,1)_s$	1021.73231(2)	0.6403(41)
$^{Q}R(3,3)_s$	1041.00824(2)	0.7127(42)
$^{Q}R(3,2)_s$	1041.05005(2)	0.5824(41)
$^{Q}R(3,1)_s$	1041.07947(2)	0.6940(41)
$^{Q}R(3,0)_s$	1041.08999(1)	1.4145(43)
$^{Q}R(4,4)_s$	1060.16208(4)	0.3043(41)
$^{Q}R(4,3)_s$	1060.20383(1)	0.9312(43)
$^{Q}R(4,2)_s$	1060.24729(2)	0.5368(41)
$^{Q}R(4,1)_s$	1060.27642(2)	0.5951(40)
$^{Q}R(5,5)_s$	1079.16159(6)	0.2267(41)
$^{Q}R(5,4)_s$	1079.19628(4)	0.3360(41)
$^{Q}R(5,3)_s$	1079.24423(2)	0.7982(42)
$^{Q}R(5,2)_s$	1079.28812(3)	0.4445(40)
$^{Q}R(5,1)_s$	1079.31799(3)	0.4427(39)
$^{Q}R(5,0)_s$	1079.32876(1)	0.8787(41)
$^{Q}R(6,6)_s$	1098.00495(4)	0.3363(42)
$^{Q}R(6,5)_s$	1098.02116(5)	0.2465(41)
$^{Q}R(6,4)_s$	1098.06641(4)	0.2930(41)
$^{Q}R(6,3)_s$	1098.11528(2)	0.5883(41)
$^{Q}R(6,2)_s$	1098.16908(4)	0.3130(39)
$^{Q}R(6,1)_s$	1098.20062(4)	0.3011(39)
$^{Q}R(7,6)_s$	1116.67826(4)	0.3134(41)
$^{Q}R(7,7)_s$	1116.69173(12)	0.1110(41)
$^{Q}R(7,5)_s$	1116.71339(6)	0.2091(40)
$^{Q}R(7,4)_s$	1116.77091(7)	0.1788(40)
$^{Q}R(7,3)_s$	1116.83586(3)	0.3593(40)
$^{Q}R(7,2)_s$	1116.88802(6)	0.1742(39)
$^{Q}R(7,1)_s$	1116.92086(12)	0.1220(67)
$^{Q}R(7,0)_s$	1116.93312(4)	0.3679(68)
$^{Q}R(8,7)_s$	1135.16530(13)	0.0958(41)
$^{Q}R(8,6)_s$	1135.18211(6)	0.2093(41)
$^{Q}R(8,8)_s$	1135.22077(18)	0.0736(41)
$^{Q}R(8,5)_s$	1135.23758(11)	0.1216(41)
$^{Q}R(8,4)_s$	1135.30880(12)	0.0984(39)
$^{Q}R(8,3)_s$	1135.36813(6)	0.1899(39)

${}^{Q}R(8,2)_s$	1135.44280(11)	0.0997(38)
${}^{Q}R(8,1)_s$	1135.47780(11)	0.1007(38)
${}^{Q}R(9,7)_s$	1153.47032(19)	0.0635(40)
${}^{Q}R(9,8)_s$	1153.48150(19)	0.0646(40)
${}^{Q}R(9,6)_s$	1153.51766(11)	0.1121(40)
${}^{Q}R(9,9)_s$	1153.58903(82)	0.0264(69)
${}^{Q}R(9,5)_s$	1153.59263(18)	0.1125(60)
${}^{Q}R(9,4)_s$	1153.67878(22)	0.0556(40)
${}^{Q}R(9,3)_s$	1153.76759(11)	0.1078(40)
${}^{Q}R(9,2)_s$	1153.83130(23)	0.0538(40)
${}^{Q}R(9,1)_s$	1153.86659(27)	0.0465(40)
${}^{Q}R(9,0)_s$	1153.87967(12)	0.0994(40)
${}^{Q}R(10,8)_s$	1171.57572(48)	0.0269(41)
${}^{Q}R(10,9)_s$	1171.62476(28)	0.0446(40)
${}^{Q}R(10,6)_s$	1171.68295(21)	0.0592(40)
${}^{Q}R(10,5)_s$	1171.78064(54)	0.0233(40)
${}^{Q}R(10,10)_s$	1171.80462(93)	0.0149(41)
${}^{Q}R(10,4)_s$	1171.87781(45)	0.0283(40)
${}^{Q}R(10,3)_s$	1171.94251(34)	0.0370(40)
${}^{Q}R(11,9)_s$	1189.49673(36)	0.0361(41)

Table S7. Measured parameters at 296 K for lines (labelled ${}^{\Delta K}\Delta J(J'',K'')_{i''}$) of the transition $\nu_4(a) \leftarrow \nu_2(a)$. The numbers in parentheses are 1σ uncertainties in the units of the last digit listed. Missing entries indicate a lack of convergence for a given parameter, which was set to zero in the final solution. An asterisk (*) indicates that the line parameter was fixed to its value in HITRAN 2020.

Line	$\boldsymbol{\nu_0}$ cm-1	$\boldsymbol{S} \times 10^{21}$ cm-1 / (mol. cm-2))	$\boldsymbol{\gamma^0_{air}}$ cm-1/atm	$\boldsymbol{\gamma^0_{self}}$ cm-1/atm
${}^{P}Q(6,4)_a$	686.483710(235)	0.0636(59)	0.0946*	0.510*
${}^{P}Q(6,5)_a$	688.443851(216)	0.0707(60)	0.1003*	0.591*
${}^{P}Q(7,3)_a$	689.250779(203)	0.0694(57)	0.0818*	0.388*
${}^{P}Q(6,6)_a$	690.177528(526)	0.0529(128)	0.1062*	0.676*
${}^{P}Q(7,6)_a$	694.219736(148)	0.1041(60)	0.0994*	0.595*
${}^{R}R(1,1)_a$	694.467574(152)	0.0933(58)	0.1028*	0.437*
${}^{P}Q(8,6)_a$	698.939503(243)	0.0625(59)	0.0921*	0.518*
${}^{P}R(1,1)_a$	704.595358(149)	0.0969(58)	0.1028*	0.437*
${}^{R}R(2,2)_a$	710.322216(72)	0.2057(60)	0.1023*	0.496*
${}^{R}R(2,1)_a$	715.916691(83)	0.1706(58)	0.0976*	0.396*
${}^{R}R(2,0)_a$	724.014362(19)	0.7277(61)	0.0931*	0.302*
${}^{R}R(3,3)_a$	726.250939(27)	0.5861(63)	0.1017*	0.541*
${}^{P}R(2,1)_a$	726.631919(71)	0.2014(58)	0.0976*	0.396*
${}^{P}R(2,2)_a$	730.268092(200)	0.0764(59)	0.1023*	0.496*
${}^{R}R(3,2)_a$	732.530959(49)	0.3026(60)	0.0967*	0.448*
${}^{R}R(3,1)_a$	737.488374(89)	0.1578(58)	0.0919*	0.360*
${}^{R}R(4,4)_a$	742.296689(39)	0.4076(62)	0.1011*	0.573*
${}^{R}R(4,3)_a$	749.256511(17)	0.9164(64)	0.0957*	0.486*
${}^{P}R(3,1)_a$	749.654478(42)	0.3389(59)	0.0919*	0.360*
${}^{P}R(3,2)_a$	752.791867(96)	0.1557(59)	0.0967*	0.448*
${}^{R}R(4,2)_a$	754.893586(42)	0.3499(60)	0.0905*	0.404*
${}^{P}R(3,3)_a$	755.873778(139)	0.1121(60)	0.1017*	0.541*
${}^{R}R(5,5)_a$	758.494328(33)	0.4943(63)	0.1003*	0.591*
${}^{R}R(4,1)_a$	759.045124(112)	0.1254(57)	0.0855*	0.327*
${}^{R}R(5,4)_a$	766.180044(27)	0.5874(63)	0.0946*	0.510*
${}^{R}R(5,3)_a$	772.397166(15)	1.0095(91)	0.0985(65)	0.418(29)
${}^{R}R(4,0)_a$	772.494903(14)	1.0715(89)	0.0778(43)	0.303(25)
${}^{P}R(4,1)_a$	773.685368(34)	0.4248(59)	0.0855*	0.327*
${}^{R}R(6,6)_a$	774.875035(16)	1.0659(93)	0.1014(64)	0.530(29)
${}^{P}R(4,2)_a$	776.176516(59)	0.2502(59)	0.0905*	0.404*
${}^{R}R(5,2)_a$	777.257159(44)	0.3299(59)	0.0837*	0.364*
${}^{P}R(4,3)_a$	778.802708(67)	0.2309(60)	0.0957*	0.486*
${}^{R}R(5,1)_a$	780.557380(145)	0.1002(59)	0.0786*	0.299*
${}^{R}R(6,5)_a$	783.345198(25)	0.6310(63)	0.0933*	0.521*
${}^{R}R(6,4)_a$	790.159163(27)	0.5804(62)	0.0875*	0.452*
${}^{R}R(7,7)_a$	791.414928(34)	0.4866(63)	0.0984*	0.585*
${}^{R}R(6,3)_a$	795.539755(19)	0.8277(63)	0.0818*	0.388*

$^{P}R(5,1)_a$	798.640569(36)	0.4044(59)	0.0786*	0.299*
$^{R}R(6,2)_a$	799.546302(67)	0.2153(58)	0.0763*	0.328*
$^{P}R(5,2)_a$	800.459043(53)	0.2793(59)	0.0837*	0.364*
$^{R}R(7,6)_a$	800.733010(14)	1.1661(92)	0.0777(40)	0.456(26)
$^{R}R(6,1)_a$	802.041902(214)	0.0670(57)	0.0710*	0.274*
$^{P}R(5,3)_a$	802.638877(46)	0.3323(61)	0.0890*	0.435*
$^{P}R(5,4)_a$	804.798139(185)	0.0850(60)	0.0946*	0.510*
$^{R}R(7,5)_a$	808.234985(28)	0.5599(62)	0.0858*	0.455*
$^{R}R(9,9)_a$	814.013035(101)	0.2057(71)	0.1044*	0.500*
$^{R}R(7,4)_a$	814.179608(33)	0.4575(61)	0.0798*	0.397*
$^{R}R(8,7)_a$	818.242385(36)	0.4475(62)	0.0906*	0.500*
$^{R}R(7,3)_a$	818.686401(24)	0.6427(61)	0.0739*	0.344*
$^{R}R(7,2)_a$	821.768971(89)	0.1612(58)	0.0683*	0.296*
$^{R}R(6,0)_a$	823.945633(20)	0.7066(60)	0.0659*	0.224*
$^{P}R(6,1)_a$	824.396700(44)	0.3274(58)	0.0710*	0.274*
$^{P}R(6,2)_a$	825.612459(57)	0.2581(59)	0.0763*	0.328*
$^{R}R(8,6)_a$	826.549535(18)	0.8564(90)	0.0783(63)	0.348(33)
$^{P}R(6,3)_a$	826.900654(48)	0.3197(60)	0.0818*	0.388*
$^{P}R(6,4)_a$	828.888983(196)	0.0814(59)	0.0875*	0.452*
$^{R}R(10,10)_a$	829.730555(607)	0.0268(60)	0.0906*	0.500*
$^{R}R(9,7)_a$	830.039564(89)	0.1806(61)	0.0906*	0.500*
$^{R}R(9,6)_a$	837.269720(45)	0.3596(62)	0.0841*	0.500*
$^{R}R(10,9)_a$	838.626241(103)	0.1564(61)	0.1044*	0.500*
$^{R}R(9,4)_a$	849.482820(105)	0.1545(61)	0.0715*	0.500*
$^{P}R(7,1)_a$	850.836478(42)	0.2227(37)	0.0629*	0.253*
$^{P}R(7,2)_a$	851.557756(52)	0.1821(37)	0.0683*	0.296*
$^{P}R(7,3)_a$	852.586684(4)	0.2523(38)	0.0739*	0.344*
$^{P}R(7,4)_a$	853.686675(10)	0.1030(38)	0.0798*	0.397*
$^{R}R(9,3)_a$	854.396331(3)	0.3360(40)	0.0655*	0.500*
$^{P}R(7,5)_a$	855.076874(21)	0.0498(38)	0.0858*	0.455*
$^{R}R(10,7)_a$	855.106313(23)	0.0476(39)	0.0906*	0.500*
$^{P}R(7,6)_a$	856.461149(30)	0.0367(39)	0.0920*	0.518*
$^{R}R(10,6)_a$	862.255542(9)	0.1128(39)	0.0841*	0.500*
$^{R}R(11,9)_a$	864.035925(20)	0.0545(39)	0.1044*	0.500*
$^{R}R(10,5)_a$	868.612563(17)	0.0625(39)	0.0777*	0.500*
$^{R}R(10,4)_a$	874.177716(21)	0.0519(39)	0.0715*	0.500*
$^{R}R(8,0)_a$	877.760175(3)	0.2894(37)	0.0488*	0.210*
$^{P}R(8,1)_a$	877.860154(7)	0.1314(37)	0.0542*	0.237*
$^{R}R(10,3)_a$	878.951187(12)	0.0877(39)	0.0655*	0.500*
$^{P}R(8,4)_a$	879.163696(19)	0.0524(37)	0.0715*	0.347*
$^{P}R(8,3)_a$	880.416402(10)	0.1009(37)	0.0655*	0.305*
$^{P}R(8,6)_a$	881.147304(19)	0.0560(38)	0.0841*	0.444*
$^{P}R(9,3)_a$	905.476415(8)	0.1271(36)	0.0655*	0.500*
$^{R}R(10,0)_a$	933.419920(15)	0.0674(36)	0.0488*	0.519*
$^{P}R(10,3)_a$	933.459364(25)	0.0654(45)	0.0655*	0.500*

Table S8. Measured parameters at 296 K for lines (labelled $^{\Delta K}\Delta J(J'',K'')_{i''}$) of the transition $\nu_2 + \nu_4(s) \leftarrow \nu_4(a)$. The numbers in parentheses are 1σ uncertainties in the units of the last digit listed. Missing entries indicate a lack of convergence for a given parameter, which was set to zero in the final solution. An asterisk (*) indicates that the line parameter was fixed to its value in HITRAN 2020.

Line	$\boldsymbol{\nu_0}$ cm^{-1}	$\boldsymbol{S} \times 10^{21}$ cm^{-1} / (mol. cm^{-2}))	$\boldsymbol{\gamma^0_{air}}$ cm^{-1}/atm	$\boldsymbol{\gamma^0_{self}}$ cm^{-1}/atm
$^{Q}P(5,1)_a$	808.855115(341)	0.0441(58)	0.0855*	0.327*
$^{Q}P(5,2)_a$	813.158688(300)	0.0513(59)	0.0905*	0.404*
$^{Q}P(4,2)_a$	832.768051(225)	0.0707(60)	0.0967*	0.448*
$^{Q}P(4,1)_a$	834.296317(184)	0.0831(58)	0.0919*	0.360*
$^{Q}P(3,1)_a$	849.957121(164)	0.0957(59)	0.0976*	0.396*
$^{Q}P(3,2)_a$	852.543884(136)	0.0770(39)	0.1023*	0.496*
$^{Q}P(2,1)_a$	872.668144(211)	0.0502(38)	0.1028*	0.437*
$^{Q}Q(7,7)_a$	901.001031(111)	0.0970(38)	0.1057*	0.673*
$^{Q}Q(6,6)_a$	904.136150(150)	0.0724(38)	0.1062*	0.676*
$^{Q}Q(5,5)_a$	906.731071(108)	0.1001(38)	0.1066*	0.664*
$^{Q}Q(8,8)_a$	908.290067(96)	0.1125(38)	0.1051*	0.657*
$^{Q}Q(4,4)_a$	908.829432(48)	0.2153(56)	0.1070*	0.581(91)

${}^{Q}Q(7,7)_a$	909.945051(125)	0.0873(38)	0.1057*	0.673*
${}^{Q}Q(5,4)_a$	910.114236(94)	0.1105(37)	0.1011*	0.573*
${}^{Q}Q(3,3)_a$	910.485453(103)	0.1029(37)	0.1072*	0.600*
${}^{Q}Q(9,8)_a$	910.841886(218)	0.0476(36)	0.0974*	0.500*
${}^{Q}Q(6,6)_a$	911.298341(100)	0.1091(38)	0.1062*	0.676*
${}^{Q}Q(6,4)_a$	911.668922(225)	0.0462(36)	0.0946*	0.510*
${}^{Q}Q(2,2)_a$	911.746606(121)	0.0853(37)	0.1073*	0.548*
${}^{Q}Q(1,1)_a$	911.925922(126)	0.0793(36)	0.1073*	0.481*
${}^{Q}Q(4,3)_a$	912.328688(174)	0.0607(37)	0.1017*	0.541*
${}^{Q}Q(5,5)_a$	912.350869(44)	0.2307(55)	0.1066*	0.499(82)
${}^{Q}Q(4,4)_a$	913.105446(84)	0.1271(38)	0.1070*	0.639*
${}^{Q}Q(7,6)_a$	913.127105(283)	0.0385(37)	0.0994*	0.595*
${}^{Q}Q(3,3)_a$	913.562078(75)	0.1410(37)	0.1072*	0.600*
${}^{Q}Q(1,1)_a$	913.584709(93)	0.1079(36)	0.1073*	0.481*
${}^{Q}Q(2,2)_a$	913.720871(56)	0.1838(37)	0.1073*	0.548*
${}^{Q}Q(6,5)_a$	913.856409(93)	0.1130(37)	0.1003*	0.591*
${}^{Q}Q(3,2)_a$	914.378975(110)	0.0918(36)	0.1023*	0.496*
${}^{Q}Q(4,3)_a$	914.481055(133)	0.0776(37)	0.1017*	0.541*
${}^{Q}Q(4,2)_a$	915.115826(220)	0.0462(36)	0.0967*	0.448*
${}^{Q}R(1,1)_a$	954.123402(98)	0.1020(36)	0.1028*	0.437*
${}^{Q}R(1,0)_a$	954.585037(194)	0.0531(39)	0.0984*	0.331*
${}^{Q}R(2,1)_a$	974.370045(79)	0.1426(57)	0.0976*	0.689(149)
${}^{Q}R(2,0)_a$	975.515417(121)	0.0722(33)	0.0931*	0.076*
${}^{Q}R(2,2)_a$	975.555964(105)	0.0943(36)	0.1023*	0.372*
${}^{Q}R(2,1)_a$	975.807770(125)	0.0824(36)	0.0976*	0.457*
${}^{Q}R(3,3)_a$	993.832103(336)	0.0348(38)	0.1017*	0.637*
${}^{Q}R(3,2)_a$	993.960139(151)	0.0591(34)	0.0967*	0.112*
${}^{Q}R(3,1)_a$	995.542087(70)	0.1536(37)	0.0919*	0.552*
${}^{Q}R(3,0)_a$	996.436877(120)	0.0730(33)	0.0872*	0.046*
${}^{Q}R(3,2)_a$	996.726860(77)	0.1335(37)	0.0967*	0.437*
${}^{Q}R(3,1)_a$	996.852378(121)	0.0733(34)	0.0919*	0.090*
${}^{Q}R(4,4)_a$	1012.147873(220)	0.0545(40)	0.1011*	0.573*
${}^{Q}R(4,2)_a$	1014.825484(187)	0.0602(39)	0.0905*	0.404*
${}^{Q}R(4,1)_a$	1016.747190(92)	0.1160(38)	0.0855*	0.327*
${}^{Q}R(4,0)_a$	1017.211088(179)	0.0587(37)	0.0807*	0.255*
${}^{Q}R(4,3)_a$	1017.308422(182)	0.0635(39)	0.0957*	0.486*
${}^{Q}R(4,1)_a$	1017.833738(187)	0.0580(38)	0.0855*	0.327*
${}^{Q}R(4,2)_a$	1017.868494(101)	0.1093(39)	0.0905*	0.404*
${}^{Q}R(5,4)_a$	1033.470060(146)	0.0816(40)	0.0946*	0.510*
${}^{Q}R(5,5)_a$	1035.868309(185)	0.0667(40)	0.1003*	0.591*
${}^{Q}R(5,1)_a$	1036.492768(134)	0.0801(38)	0.0786*	0.299*
${}^{Q}R(5,2)_a$	1039.006387(125)	0.0888(38)	0.0837*	0.364*
${}^{Q}R(6,4)_a$	1054.841363(231)	0.0511(39)	0.0875*	0.452*
${}^{Q}R(6,5)_a$	1057.537354(205)	0.0590(40)	0.0933*	0.521*
${}^{Q}R(6,1)_a$	1059.510707(194)	0.0561(38)	0.0710*	0.274*
${}^{Q}R(6,2)_a$	1059.711056(184)	0.0608(38)	0.0763*	0.328*

Table S9. Measured parameters at 296 K for lines (labelled ${}^{\Delta K}\Delta J(J'',K'')_{i''}$) of the transition $\nu_2 + \nu_4(a) \leftarrow \nu_4(s)$. The numbers in parentheses are 1σ uncertainties in the units of the last digit listed. Missing entries indicate a lack of convergence for a given parameter, which was set to zero in the final solution. An asterisk (*) indicates that the line parameter was fixed to its value in HITRAN 2020.

Line	$\boldsymbol{\nu_0}$ cm-1	$\boldsymbol{S} \times 10^{21}$ cm-1 / (mol. cm-2))	$\boldsymbol{\gamma^0_{air}}$ cm-1/atm	$\boldsymbol{\gamma^0_{self}}$ cm-1/atm
${}^{Q}P(5,2)_s$	857.260297(180)	0.0569(38)	0.0905*	0.404*
${}^{Q}P(5,1)_s$	858.452124(165)	0.0600(37)	0.0855*	0.327*
${}^{Q}P(4,1)_s$	876.498087(114)	0.0857(56)	0.0308(98)	0.272(207)
${}^{Q}P(4,2)_s$	878.003201(159)	0.0668(38)	0.0967*	0.448*
${}^{Q}P(3,2)_s$	898.631566(162)	0.0664(39)	0.1023*	0.496*
${}^{Q}P(3,1)_s$	899.252473(135)	0.0763(38)	0.0976*	0.396*
${}^{Q}P(2,1)_s$	918.362122(160)	0.0632(36)	0.1028*	0.437*
${}^{Q}Q(9,9)_s$	953.776312(214)	0.0488(37)	0.1044*	0.500*
${}^{Q}Q(8,7)_s$	954.485395(190)	0.0568(37)	0.0985*	0.585*
${}^{Q}Q(8,8)_s$	955.595190(118)	0.0944(38)	0.1051*	0.657*
${}^{Q}Q(7,7)_s$	955.944105(88)	0.1270(38)	0.1057*	0.673*

${}^{Q}Q(7,7)_s$	956.508401(143)	0.0781(38)	0.1057*	0.673*
${}^{Q}Q(6,5)_s$	956.796250(110)	0.0978(37)	0.1003*	0.591*
${}^{Q}Q(6,6)_s$	956.859464(134)	0.0834(38)	0.1062*	0.676*
${}^{Q}Q(6,6)_s$	957.285248(98)	0.1136(38)	0.1062*	0.676*
${}^{Q}Q(5,4)_s$	957.499623(89)	0.1201(37)	0.1011*	0.573*
${}^{Q}Q(5,5)_s$	957.659494(109)	0.1026(38)	0.1066*	0.664*
${}^{Q}Q(4,4)_s$	957.827269(117)	0.0962(39)	0.1070*	0.639*
${}^{Q}Q(5,5)_s$	957.883395(54)	0.2067(38)	0.1066*	0.664*
${}^{Q}Q(4,3)_s$	958.259890(174)	0.0607(37)	0.1017*	0.541*
${}^{Q}Q(4,4)_s$	958.340748(49)	0.2277(57)	0.0889(169)	0.676(93)
${}^{Q}Q(4,2)_s$	958.844830(182)	0.0559(36)	0.0967*	0.448*
${}^{Q}Q(3,3)_s$	958.903456(100)	0.1081(38)	0.1072*	0.600*
${}^{Q}Q(3,2)_s$	959.279130(123)	0.0841(37)	0.1023*	0.496*
${}^{Q}Q(2,2)_s$	959.342942(140)	0.0757(37)	0.1073*	0.548*
${}^{Q}Q(3,3)_s$	959.494012(98)	0.1110(38)	0.1072*	0.600*
${}^{Q}Q(2,2)_s$	959.629244(57)	0.1852(38)	0.1073*	0.548*
${}^{Q}Q(1,1)_s$	960.238306(118)	0.0866(37)	0.1073*	0.481*
${}^{Q}R(1,1)_s$	999.487531(147)	0.0610(34)	0.1028*	0.109*
${}^{Q}R(1,0)_s$	1000.145480(189)	0.0565(38)	0.0984*	0.331*
${}^{Q}R(2,0)_s$	1020.133272(174)	0.0621(38)	0.0931*	0.302*
${}^{Q}R(2,1)_s$	1020.141325(239)	0.0467(39)	0.0976*	0.396*
${}^{Q}R(2,2)_s$	1020.276756(121)	0.0966(40)	0.1023*	0.496*
${}^{Q}R(2,1)_s$	1020.706088(76)	0.1451(39)	0.0976*	0.396*
${}^{Q}R(3,1)_s$	1038.443298(81)	0.1366(39)	0.0919*	0.360*
${}^{Q}R(3,2)_s$	1039.088451(201)	0.0573(39)	0.0967*	0.448*
${}^{Q}R(3,1)_s$	1039.955035(170)	0.0662(38)	0.0919*	0.360*
${}^{Q}R(3,0)_s$	1040.023149(136)	0.0786(38)	0.0872*	0.277*
${}^{Q}R(3,2)_s$	1040.120748(100)	0.1144(39)	0.0967*	0.448*
${}^{Q}R(4,2)_s$	1058.181125(248)	0.0466(39)	0.0905*	0.404*
${}^{Q}R(4,4)_s$	1058.940682(159)	0.0769(40)	0.1011*	0.573*
${}^{Q}R(4,1)_s$	1059.631082(233)	0.0479(38)	0.0855*	0.327*
${}^{Q}R(4,0)_s$	1059.776151(240)	0.0449(38)	0.0807*	0.255*
${}^{Q}R(4,2)_s$	1059.853917(98)	0.1162(39)	0.0905*	0.404*
${}^{Q}R(4,1)_s$	1060.230915(90)	0.1224(38)	0.0855*	0.327*
${}^{Q}R(5,1)_s$	1076.597537(131)	0.0842(38)	0.0786*	0.299*
${}^{Q}R(5,4)_s$	1077.859646(198)	0.0614(40)	0.0946*	0.510*
${}^{Q}R(5,5)_s$	1078.553761(265)	0.0478(41)	0.1003*	0.591*
${}^{Q}R(5,2)_s$	1079.429437(150)	0.0761(39)	0.0837*	0.364*
${}^{Q}R(6,4)_s$	1096.447987(201)	0.0595(40)	0.0875*	0.452*
${}^{Q}R(6,5)_s$	1097.508834(299)	0.0418(40)	0.0933*	0.521*
${}^{Q}R(6,1)_s$	1098.844576(221)	0.0507(38)	0.0710*	0.274*
${}^{Q}R(6,2)_s$	1098.922136(168)	0.0677(39)	0.0763*	0.328*